Taylor & Francis
Taylor & Francis Group

Journal of the Air & Waste Management Association

ISSN: 1096-2247 (Print) 2162-2906 (Online) Journal homepage: www.tandfonline.com/journals/uawm20

Analysis and updates to the IMPROVE Equation for estimating light extinction

Bonne Ford, Anthony J. Prenni, William Malm, Scott A. Copeland, Bret A. Schichtel & Jenny Hand

To cite this article: Bonne Ford, Anthony J. Prenni, William Malm, Scott A. Copeland, Bret A. Schichtel & Jenny Hand (29 Apr 2026): Analysis and updates to the IMPROVE Equation for estimating light extinction, Journal of the Air & Waste Management Association, DOI: 10.1080/10962247.2026.2651554

To link to this article: https://doi.org/10.1080/10962247.2026.2651554

JOURNAL OF THE AIR & WASTE MANAGEMENT ASSOCIATION
https://doi.org/10.1080/10962247.2026.2651554

Taylor & Francis
Taylor & Francis Group

TECHNICAL PAPER

Analysis and updates to the IMPROVE Equation for estimating light extinction

Bonne Ford[a], Anthony J. Prenni[b], William Malm[a], Scott A. Copeland[a], Bret A. Schichtel[b], and Jenny Hand[a]

[a]Cooperative Institute for Research in the Atmosphere, Colorado State University, Fort Collins, CO, USA; [b]National Park Service, Cooperative Institute for Research in the Atmosphere, Colorado State University, Fort Collins, CO, USA

ABSTRACT

The Clean Air Act Amendments of 1977 included protections for visibility in Class I areas, such as national parks and wilderness areas. Visibility degradation (haze) is determined from speciated aerosol mass concentrations measured by the Interagency Monitoring of Protected Visual Environments (IMPROVE) network. Mass concentrations are converted into reconstructed light extinction values using an algorithm that considers the mass extinction efficiencies (MSEs) and water uptake of different major aerosol species. This algorithm is evaluated against measured light scattering (b_{sp}) using nephelometers that are co-located at several IMPROVE sites. Evaluating the performance of the algorithm is critical because of its use in tracking visibility trends for the U.S. Environmental Protection Agency's (EPA's) Regional Haze Rule (RHR). Previous evaluations (2001–2016) demonstrated that the current IMPROVE reconstructed light extinction equation (Second IMPROVE Equation) suggested in the RHR guidance results in spatial and temporal biases in visibility trends, leading to greater uncertainty in reaching national visibility goals. Extending the evaluation through 2024 suggests that using the current algorithm continues to introduce biases in visibility trends, primarily due to the parameterized dependence of MSEs on mass concentrations in the equation. We recommend a revised algorithm (Third IMPROVE Equation) that removes this MSE-mass dependence and updates aerosol composition assumptions to be consistent with the most recent science. The equation is more appropriate for representing long-term trends in regulatory visibility metrics across the IMPROVE network.

Implications: IMPROVE data are central to the EPA's Regional Haze Rule (RHR) for tracking visibility trends in Class I areas. The current light-extinction equation (Second IMPROVE Equation) improved fits with early 2000s measurement data but introduced long-term biases. We present a revised equation, based on the First IMPROVE Equation, that improves consistency with measured light scattering and long-term trends. Implementing the revision would minimally affect RHR tracking metrics. This work provides timely input to ongoing EPA evaluations of RHR metrics and implementation guidance.

PAPER HISTORY
Received November 12, 2025
Revised February 12, 2026
Accepted March 17, 2026

Introduction

Particulate and gaseous air pollution can degrade visibility, which is a protected resource for Class I areas (CIAs) in the United States under the 1977 Clean Air Act Amendments (CAAA). CIAs are large national parks (greater than 6,000 acres) and wilderness areas (greater than 5,000 acres) that existed when the CAAA were enacted and were designated as such to preserve and improve visual air quality. The Interagency Monitoring of Protected Visual Environments (IMPROVE) program has been monitoring speciated particulate matter at sites representative of visibility-protected CIAs since 1988 (Malm et al. 1994). Data are used to support the U.S. Environmental Protection Agency's (EPA's) Regional Haze Rule (RHR) by tracking progress toward the goal of no human impairment of visibility in CIAs by 2064 (U.S. Environmental Protection Agency 1999).

The RHR metrics used to track progress are based on an equation to estimate the light extinction coefficient (*bext*) from speciated aerosol mass concentrations. The b_{ext} is the sum of scattering by gases (b_{sg}) and particles (b_{sp}), and absorption by gases (b_{ag}) and particles (b_{ap}). The b_{ext} due to gases is directly estimated if gas concentrations are measured; however, calculating b_{ext} due to particles requires more information, such as the composition and size of the different particles. The general form of a reconstructed b_{ext} algorithm for particles is $b_{ext} = \Sigma MSE \cdot M \cdot f(RH)$ and assumes an externally mixed aerosol model (Malm et al. 1994; Hand and Malm 2007). For each major aerosol species, M is the mass concentration, MSE is the dry mass scattering efficiency (i.e., the change in scattering per unit mass concentration),

CONTACT Bonne Ford bonne.ford@colostate.edu Cooperative Institute for Research in the Atmosphere, Colorado State University, 1375 Campus Delivery, Fort Collins, CO, USA.

Supplemental data for this article can be accessed online at https://doi.org/10.1080/10962247.2026.2651554.

and *f(RH)* is the water growth curve, which is composition-dependent and a function of relative humidity (RH). The *f(RH)* is determined from the ratio of b_{sp} under humid conditions ($b_{sp,RH}$) to b_{sp} under dry conditions ($b_{sp,dry}$) ($f(RH)=b_{sp,RH}/b_{sp,dry}$). MSE is calculated using Mie theory with an assumed aerosol size distribution and composition.

Historically, tracking progress in visibility for the RHR has relied on two forms of a reconstructed b_{ext} equation. The 2003 RHR Guidance applied what is often referred to as the "First IMPROVE Equation" (U.S. EPA 2003), which followed the general form of the equation described above and included contributions from major aerosol species such as ammonium sulfate (AS), ammonium nitrate (AN), organic carbon mass (OM), elemental carbon, fine soil (dust), and coarse particle mass. Pitchford et al. (2007) identified issues with the First IMPROVE Equation that resulted in biases for low and high measured and calculated b_{sp}, and therefore proposed a revised equation ("Second IMPROVE Equation") that was designed to account for these biases. The Second IMPROVE Equation is suggested in the current RHR guidance (EPA 2018). The major difference between these two equations is the assumption regarding the size distribution of the aerosol; the First IMPROVE Equation assumes a single size mode for fine species, while the Second IMPROVE Equation assumes two size modes. The MSEs corresponding to these two size distributions in the Second IMPROVE Equation are scaled to mass concentrations (Figure S1). Other assumptions regarding mass composition were also updated in the Second IMPROVE Equation to align with the current science at the time of its derivation (Pitchford et al. 2007). The Second IMPROVE Equation performed well for the 2000–2004 period used in its development, reducing the biases at high and low extinction values (Pitchford et al. 2007). However, it was found that the Second IMPROVE Equation caused biases in visibility trends for later years, particularly in the eastern U.S. (Lowenthal et al. 2015; Prenni et al. 2019). These biases in trends were attributed to the assumptions used in the parameterization that scaled MSEs to mass concentrations. Based on these biases with the Second Equation, progress toward RHR goals is likely overestimated. In fact, Hand et al. (2020) reported that decreasing trends in b_{ext} could be overestimated by 1% yr^{-1} in the eastern U.S. and 0.5% yr^{-1} in the western U.S., emphasizing the need for an equation that accurately reproduces visibility trends.

The main purpose of this paper is to develop a new (Third) IMPROVE Equation to resolve the biased visibility trends. In doing so, we summarize the performance of the First and Second IMPROVE Equations against the most recent b_{sp} nephelometer measurements, following the evaluation by Prenni et al. (2019). The new equation follows the framework of the First IMPROVE Equation, although with updated assumptions regarding mass concentrations and *f(RH)*.

The IMPROVE network

At the time of this study, there were 155 IMPROVE sites, of which 110 were termed "IMPROVE RHR sites" that were used to report visibility trends for 155 of the 156 CIAs with visibility protection (the exception being the Bering Sea Wilderness). All IMPROVE sites are equipped with filter-based particle samplers. Several sites throughout the network are also equipped with integrating nephelometers for direct measurements of b_{sp} (11 sites at the time of this study). More information on IMPROVE site locations can be found in Hand (2023). All IMPROVE aerosol data are available from the Federal Land Manager Environmental Database (FED, https://views.cira.colostate.edu/fed).

Filter-based aerosol mass and composition measurements

The IMPROVE sampler has four modules: A, which is used for gravimetric $PM_{2.5}$ (particles with an aerodynamic diameter less than 2.5 μm) mass, elemental analysis, and filter absorption; B, which is used for ion analysis; C, which is used for carbon analysis, and D, which is used for gravimetric PM_{10} (particles with an aerodynamic diameter less than 10 μm) mass. Filters are pre-weighed (for gravimetric analysis) and pre-fired (for carbon analysis) before being sampled. Sampling is performed on a one-in-three-day schedule, collecting 24-hour samples (midnight to midnight local standard time). Historically, flow was controlled with a critical orifice controller; however, all IMPROVE sites were switched to active flow control over the period of 2023–2025. Analysis of particulate mass and composition is performed at dedicated labs, with lag times of approximately 6 months. Total mass concentrations of gravimetric $PM_{2.5}$ and PM_{10} are determined from the filter weights and sampling volume, and are reported at local ambient conditions (the term "mass" used hereafter is taken to mean "local ambient mass concentration").

Aerosol mass concentrations require assumptions regarding their molecular form in the atmosphere. Here, OM concentrations are calculated by multiplying organic carbon (OC) by a monthly-varying *Roc*, also known as the OM to OC ratio (OM/OC), as has been suggested by recent studies with IMPROVE data (Hand

2019, 2024). AS is calculated from sulfate ion concentrations multiplied by 1.375, based on the assumption that sulfate is fully neutralized by ammonium. When sulfate data are missing, AS is calculated from sulfur using a 4.125 multiplier. AN is calculated from nitrate ion concentrations multiplied by 1.29. Fine soil, or dust, is calculated from elemental species using multiplication factors to represent the normal oxides of elemental species found in soil, following Hand et al. (2019), who increased multiplication factors by 15% relative to those presented in Malm et al. (1994). Sea salt is calculated by multiplying chloride ion concentrations by 1.8; chlorine data are used when chloride ion data are missing. Coarse mass (CM) is calculated as the difference between PM_{10} and $PM_{2.5}$ mass concentrations.

Nephelometer measurements

Nephelometers and/or transmissometers co-located at a subset of IMPROVE sites (Figure 1, Table S1) have been part of the network since its inception (e.g., Malm et al. 1994; Malm and Sisler 2000) and have been critical for evaluating various forms of the IMPROVE b_{ext} algorithms (e.g., Pitchford et al. 2007; Prenni et al. 2019). From 1993 through 2023, monitoring sites operated Optec, Inc. Model NGN-2 nephelometers. In 2022, the National Park Service began replacing these instruments with Ambilabs® Two Wavelength Integrating Nephelometers (2-WIN), as the Optec NGN-2 models were no longer being supported (Malm et al. 2024). Optec b_{sp} and co-located RH data are available for download through the FED website. The 2-WIN data will be publicly available starting in 2026.

The Optec nephelometer reports hourly ambient b_{sp} at an effective wavelength of 530 nm, and the 2-WIN reports 5-minute data at 525 nm. Measured b_{sp} from both instruments are scaled to 550 nm using an Ångström exponent of one (i.e., not dominated by coarse or fine particles), as this is the assumed wavelength for the IMPROVE b_{ext} equations (e.g., Gordon et al. 2018). The Optec is an open-air instrument with no size cut and measures b_{sp} at near ambient conditions, while the 2-WIN operates with a 2.5 µm cyclone and has mild heating, which reduces the RH and may volatilize some species such as AN (Malm et al. 2024). Neither instrument measures particle absorption. We averaged the 5-minute 2-WIN data to an hourly value for comparison with Optec data. Following Prenni et al. (2019), for both instruments, we only used hourly data points with an RH of <90% and b_{sp} values less than 500 Mm^{-1} (and a data flag of V0, signifying a "Valid value" for Optec data). We required 16 hourly measurements to create a daily average. This is a higher completeness requirement than in Prenni et al. (2019) and a lower completeness criterion than Pitchford et al. (2007), but it provided good agreement between measured and calculated scattering without significantly reducing available

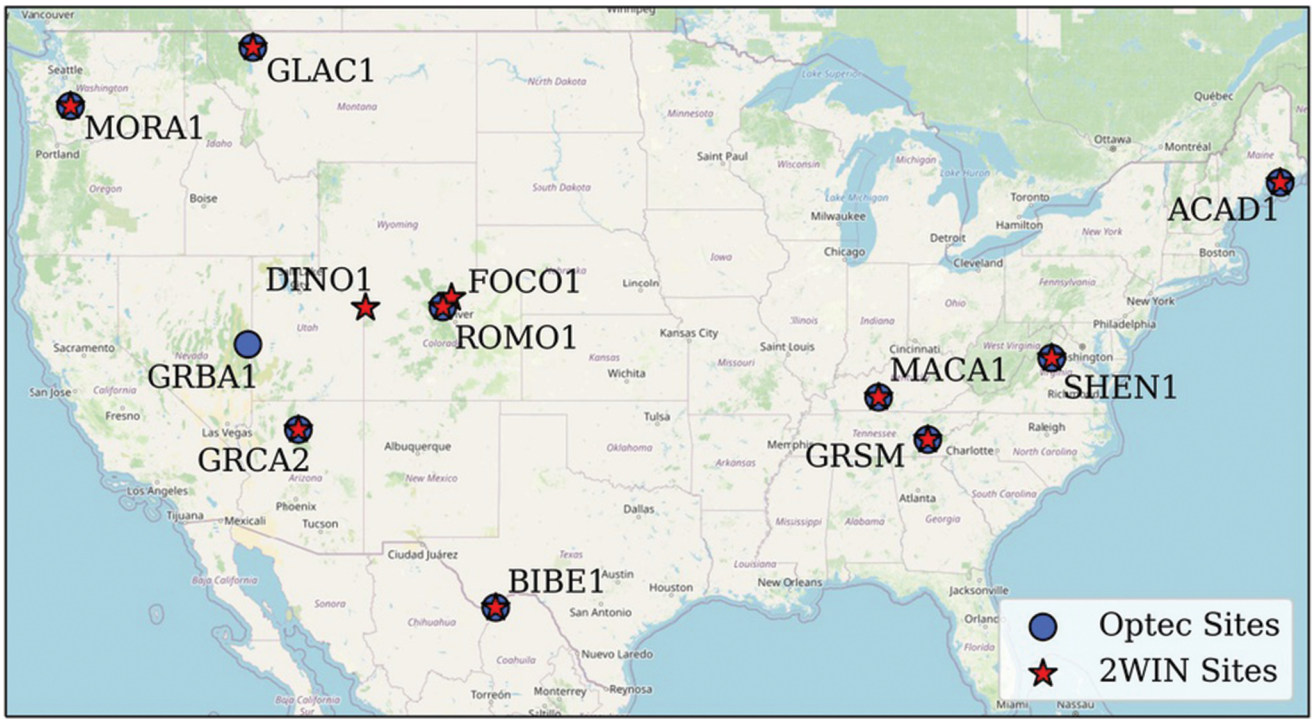

Figure 1. Location of IMPROVE sites used in this study with Optec nephelometers (blue dots) and 2-WIN nephelometers (red stars), and some sites have had both instruments. Additional site information is given in Table S1.

data (Figure S2). The Optec nephelometers have a detection limit of 1–2 Mm^{-1} and an uncertainty of ~10% at 100 Mm^{-1}, and an uncertainty of ~100–200% at 1–2 Mm^{-1} (Molenar 1997, 2000). The 2-WIN nephelometers have a detection limit of 0.14 Mm^{-1} and an uncertainty of 10% (Müller et al. 2011; Malm et al. 2024).

We also used the RH measurement from inside the nephelometers' sampling chambers to determine the hourly *f(RH)* values. These hourly *f(RH)* values were then averaged into a daily *f(RH)* value (using the same completeness criteria as above) to match the time resolution of the IMPROVE data. When calculating b_{sp} for comparison with Optec data, we reduced the CM scattering by 50% to account for the known Optec nephelometer truncation error (Malm and Hand 2007). Since the 2-WIN nephelometer operates with a 2.5 µm cyclone, CM was removed from the b_{sp} calculation for comparisons with 2-WIN data.

We also removed nephelometer data from instruments with poor calibrations. The 2-WIN nephelometers are calibrated using a span gas (CO_2) measurement, which is compared to the expected value, and a measurement of zero air. These calibrations were checked weekly, and at some sites daily, using a span check and a zero air check. We removed periods with anomalous zero measurements (z-score >3 that worsened the span check agreement) and/or anomalous span measurements (when expected and zero-corrected span checks >15%). The Optec instruments have been part of the network for a much longer time and have been systematically replaced at sites for routine maintenance or due to instrument failure. For the Optec data, which uses a refrigerant for calibration, we tested for a change in the time series between the measured and calculated b_{sp} (using the Second IMPROVE equation), which also corresponded to a noted instrumentation replacement (e.g., Figure S3). In particular, we removed data periods that corresponded to a specific instrument deployment when (1) the median ratio of the daily measured to calculated b_{sp} was greater than 1.5 or less than 0.5 (for the period of deployment), (2) the 10th, 50th, and 75th percentiles of measured b_{sp} all changed by >50% after the instrument changed, and (3) periods where the slope and intercept between measured and calculated b_{sp} fell outside the 10th–90th percentile of all slopes and intercepts across the network and across all time periods. All data from the deployment of an instrument at the given site when these changes were noted were removed from the analysis (e.g., Figure S3 shows an example). We also removed any Optec data collected after 2022, as the instruments were no longer being supported.

Optec and 2-WIN co-locations

Two of the sites in Colorado—Fort Collins (FOCO1) and Rocky Mountain National Park (ROMO1)—had periods in 2022 with both Optec and 2-WIN nephelometers running concurrently (Malm et al. 2024). At the FOCO1 site, the Optec data were higher than the 2-WIN data; the relative bias between the Optec-measured b_{sp} and calculated b_{sp} (using the Second IMPROVE Equation, eq 2) on these co-located days was −0.31 compared to −0.14 for the 2-WIN. At the ROMO1 site, the Optec nephelometer data were low compared to the 2-WIN data (Figure S4). The relative bias between the Optec-measured and calculated b_{sp} on these co-located days is 0.34 compared to −0.06 for the 2-WIN. Malm et al. (2024) investigated differences in the Optec and 2-WIN measurements at FOCO1 and found that they were primarily due to the instruments' different particle size cuts and sample heating. Scattering should be higher from the Optec nephelometer, as the RH in the Optec is higher, and coarse particles enter the Optec scattering chamber (Malm et al. 2024). At ROMO1, issues with degradation of the Optec nephelometer and poor calibration were the likely causes of the 2-WIN measured b_{sp} being larger (Malm et al. 2024). Comparisons between the $b_{sp,meas}$ and $b_{sp,calc}$ in the results sections show that the nephelometer measurements from both instruments were useful for analyzing the performance of the IMPROVE equations.

IMPROVE reconstructed extinction equations

The IMPROVE reconstructed b_{ext} equation, and the U.S. EPA's RHR guidance have evolved over time with the collection of IMPROVE measurement data and to incorporate current advances in aerosol science. The evolution of the equation is described here, along with the specific forms of the equation used in this study.

Malm et al. (1994) proposed the first iteration of the IMPROVE reconstructed b_{ext} equation that followed the general form provided in the Introduction. As stated, it included contributions from AS, AN, OM, fine soil, CM, and b_{ext} from elemental carbon. A single lognormal size distribution was assumed for AS, AN, and OM (with a mass mean diameter, *Dp*, of 0.3 µm and geometric standard deviation, σ_g, of 2.0) to calculate MSEs. The same *f(RH)* curve was used for AS and AN, and half the OM was assumed to be hygroscopic (Malm et al. 1994). The derivation and validation of this equation (e.g., Malm et al. 1994) and its subsequent iterations relied on direct measurements of b_{sp} by nephelometers (Malm et al. 1994; Lowenthal et al. 2003, 2015; Malm and Hand 2007; Pitchford et al. 2007; Prenni et al. 2019). Analysis of data collected from several IMPROVE sites with co-located optical and mass measurements (e.g., Malm et al. 1994,

1996; Malm and Pitchford 1997) led to the first modifications of the equation, primarily with respect to OM. The MSE was increased relative to AS and AN, and OM was no longer considered hygroscopic based on field studies in which organics were found to be either non-hygroscopic or very weakly hygroscopic (Malm et al. 2000; Malm and Day 2001; Lowenthal et al. 2003). This version of the equation (Table 1), referred to as the "First IMPROVE Equation" was incorporated into the 1999 RHR visibility monitoring guidance document (U.S. EPA 1999) and the 2003 RHR tracking progress guidance (U.S. EPA 2003).

However, subsequent studies showed a systematic bias between measured and calculated b_{sp}, with a positive bias at low b_{sp} and a negative bias at high b_{sp}, when applying the First IMPROVE Equation, which was of concern due to potential biases in tracking haze for the RHR (e.g., Malm et al. 2003; Lowenthal and Kumar 2004; Malm and Hand 2007; Pitchford et al. 2007). These biases were attributed to the dry MSEs used with the First IMPROVE Equation, which represented a single size distribution for each species. Studies have shown large variability in reported MSE due to changes in particle size, composition, and optical properties, as well as due to the methods used to derive them (e.g., Ames et al. 2000; Ryan et al. 2005; Hand and Malm 2007; Malm and Hand 2007), suggesting that using a single MSE value (for each species) for all sites and time periods may not be appropriate. Several studies have specifically suggested that the MSE increases with increasing aerosol mass concentrations (Ames et al. 2000; Ryan et al. 2005; Hand and Malm 2007; Malm and Hand 2007; Laing et al. 2016; Marsavin et al. 2023). Thus, a revised equation (Second IMPROVE Equation) was developed to account for this dependence by scaling the MSEs based on mass concentrations (Pitchford et al. 2007).

The development of the Second IMPROVE Equation relied on a bimodal or "split-component" model to separate $PM_{2.5}$ AS, AN, and OM into small and large size modes to represent fresh and more aged particles, respectively (Pitchford et al. 2007). The MSEs for the size modes were calculated assuming lognormal aerosol size distributions with a Dp of 0.2 μm and σ_g of 2.2 for the small mode and a Dp of 0.5 μm and σ_g of 1.5 for the large mode. The MSEs are scaled by apportioning the measured $PM_{2.5}$ mass into each size mode relative to a break point (20 μg m^{-3}) that was empirically derived (Figure S1). Pitchford et al. (2007) showed that using the Second IMPROVE equation reduced the biases for low and high b_{sp} values, particularly for sites in the eastern U.S. Current technical guidance from the EPA on tracking visibility for the RHR still relies on the Second IMPROVE equation (U.S. EPA 2018).

Table 1. Descriptions of the First and Second IMPROVE Equations used in RHR guidance and modified for evaluations in this paper.

b_{ext} component	First IMPROVE Equation as in RHR guidance (U.S. EPA 2003)	Second IMPROVE Equation as in RHR guidance (U.S. EPA 2018)	First IMPROVE Equation used in this paper	Second IMPROVE Equation used in this paper
Sea Salt	Not included	Included as in Pitchford et al. (2007) with MSE = 1.7 m^2g^{-1} (based on Quinn et al. 1995, 1996) and $f_{SS}(RH)$ (originally from Tang et al. 1997)	MSE = 1.7 m^2g^{-1} as in Pitchford et al. (2007), updated $f_{SS}(RH)$ with κ = 1.1	
Dust/Fine Soil	Mass calculated as in Malm et al. (1994), MSE = 1 m^2g^{-1} (originally from Trijonis et al. 1987)		Mass calculated as in Hand et al. (2019), MSE = 1 m^2g^{-1} (originally from Trijonis et al. 1987)	
Elemental carbon	Included as in Malm et al. (1994), mass absorption efficiency = 10 m^2g^{-1} (originally from Trijonis et al. 1987)			
Coarse Mass	Included as in Malm et al. (1994), MSE = 0.6 m^2g^{-1} (originally from Trijonis et al. 1987)			
Ammonium Sulfate (AS)	AS from sulfur, Single mode, MSE = 3 m^2g^{-1}, $f(RH)$	AS from sulfur, two modes, as in Pitchford et al. (2007), MSEs = 2.2 & 4.8 m^2g^{-1}, $f_S(RH)$ and $f_L(RH)$ for each mode	AS from sulfate ion, single mode, MSE = 3 m^2g^{-1}, updated $f_{AS}(RH)$ with κ = 0.61	AS from sulfate ion, two modes, as in Pitchford et al. (2007), MSEs = 2.2 & 4.8 m^2g^{-1}, updated $f_{AS}(RH)$ for each mode with κ = 0.61
Ammonium Nitrate (AN)	Single mode, MSE = 3 m^2 g^{-1}, use $f(RH)$ from AS	Two modes, as in Pitchford et al. (2007), MSEs = 2.4 & 5.1 m^2 g^{-1}, use $f_S(RH)$ and $f_L(RH)$ from AS for each mode	Single mode, MSE = 3 m^2g^{-1}, updated $f_{AN}(RH)$ with κ = 0.67	Two modes, as in Pitchford et al. (2007), MSEs = 2.2 & 4.8 m^2g^{-1}, updated $f_{AN}(RH)$ for each mode with κ = 0.67
Organic Matter	Roc = 1.4 (originally based on Japar et al. 1984), $f(RH)$ =1, single mode, MSE = 4 m^2 g^{-1}	Roc = 1.8, non-hygroscopic, two modes, as in Pitchford et al. (2007), MSEs = 2.8 & 6.1 m^2 g^{-1}	Roc = monthly, Hygroscopic (κ = 0.1), single mode, MSE = 4 m^2 g^{-1}	Roc = monthly, Hygroscopic (κ = 0.1), two modes as in Pitchford et al. (2007), MSEs = 2.8 & 6.1 m^2 g^{-1}
Rayleigh Scattering	Default value of 10 Mm^{-1} as in Malm et al. (1994)	Site-specific as in Pitchford et al. (2007)		

Prenni et al. (2019) demonstrated that the agreement between calculated and measured b_{sp} worsened over time, with increasingly underestimated b_{sp} when using the Second IMPROVE Equation. They attributed this deterioration to assumptions regarding apportionment of mass between the size modes in the split-component framework, specifically with the break point used to split the modes. Because of the biases identified by Prenni et al. (2019), we evaluated both the First and Second IMPROVE Equations against recent nephelometer data. Following suggestions in Prenni et al. (2019), we modified both equations to be consistent with the most current aerosol science. These modifications are described here and summarized in Table 1. While these equations represent modified versions of the "traditional" First and Second IMPROVE Equations, we refer to them only as the First and Second IMPROVE Equations throughout the rest of the paper for clarity, and we point out where they differ from the RHR guidance when necessary (Table 1). The performance of these modified equations is discussed in the Results and Discussion section.

The First IMPROVE Equation (with modifications, as detailed in Table 1) is shown in eq 1, where b_{ext} (in units of Mm^{-1}, 550 nm) is reconstructed by multiplying the mass concentrations of the six aerosol species (in units of $\mu g\ m^{-3}$) by their MSEs (or mass extinction efficiency for elemental carbon, both in units of $m^2\ g^{-1}$) and an $f(RH)$ for hygroscopic species, and then adding site-specific Rayleigh scattering (in units of Mm^{-1}). Assumptions regarding the molecular forms of the various species were discussed earlier, including modifications such as updated calculations of OM and fine soil mass (Table 1). MSEs for fine soil, CM, and elemental carbon are the same as in Malm et al. (1994) and were from a literature review by Trijonis et al. (1987). The MSEs for AS, AN, and OM are the same as in DeBell et al. (2006) and were derived using a single size distribution with a mass mean diameter of 0.3 μm and geometric standard deviation of 2.0. The modifications to the equation also include the contribution of sea salt and its water growth curve (*fss(RH)*, Figure 2(b)), derived using the size distribution in Pitchford et al. (2007), *Dp* of 2.5, σ_g of 2) and κ = 1.1 (Zieger et al. 2017), as well as a site-specific value for Rayleigh scattering. Additionally, species-specific *f(RH)* curves for AS ($f_{AS}(RH)$) and AN ($f_{AN}(RH)$) were derived using κ = 0.61 for AS and κ = 0.67 for AN (Petters and Kreidenweis 2007), for the size distributions mentioned above (Figure 2(b)). We also included a *f(RH)* for OM ($f_{OM}(RH)$, Figure 2(b)). Studies have shown that some organic aerosols are hygroscopic (Malm et al. 2005; Petters and Kreidenweis 2007; Jimenez et al. 2009; Brock et al. 2016), and evaluations of the IMPROVE b_{ext} equations by Lowenthal et al. (2015) and Lowenthal and Kumar (2016) suggested that a $f_{OM}(RH)$ curve should be implemented into the IMPROVE equation. Because OM is now a much larger fraction of the aerosol mass measured in the IMPROVE network (e.g., Hand 2024), accounting for water uptake by organics is likely more important for estimating b_{sp} and for agreement between calculated and measured b_{sp}. A κ of ~0.10 for organics has been found in many laboratory and field studies (Prenni et al. 2007;

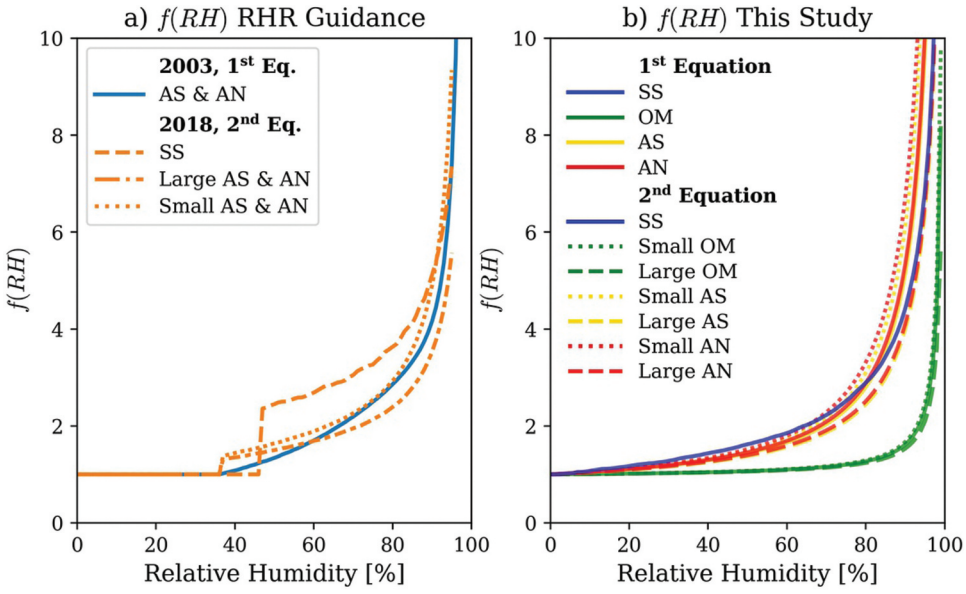

Figure 2. (a) The *f(RH)* curves in the U.S. EPA's Regional haze Rule (RHR) guidance in 2003 for use with the first equation ("2003, 1st eq"; blue) and in 2018 for use with the second equation ("2018, 2nd eq"; orange) for different species (AS: ammonium sulfate, AN: ammonium nitrate, SS: sea salt) and size modes (small and large), and (b) the *f(RH)* curves calculated for use in this study for the First and Second IMPROVE Equations for the different species (AS, AN, OM: organic matter, SS) and size modes (listed in text).

Gunthe et al. 2009; Dusek et al. 2010; Pierce et al. 2011) and is used in other modeling and data analysis studies (e.g., Pringle et al. 2010; Haslett et al. 2019; Latimer and Martin 2019). Thus, an $f_{OM}(RH)$ was derived assuming a κ of 0.1 for the size distribution mentioned above.

$$\begin{aligned} b_{ext} = {} & 3.0 \times f_{AS}(RH) \times [Ammonium\ Sulfate] + 3.0 \\ & \times f_{AN}(RH) \times [Ammonium\ Nitrate] + 4.0 \\ & \times f_{OM}(RH) \times [Organic\ Mass] + 10.0 \\ & \times [Elemental\ \text{Carbon}] + 1 \times [FineSoil] + 0.6 \\ & \times [Coarse\ Mass] + 1.7 \times f_{SS}(RH) \times [Sea\ Salt] \\ & + Rayleigh\ scattering(Site\ Specific) \end{aligned} \quad (1)$$

A comparison of *f(RH)* values applied in the "traditional" First and Second IMPROVE Equations (used in the RHR) guidance and those used in the modified equations is shown in Figure 2(a,b), respectively. The $f_{OM}(RH)$ is much lower than $f_{AS}(RH)$ and $f_{AN}(RH)$, which are also now separate curves (Figure 2(b)). These *f(RH)* curves were used for measurement comparisons as well as to determine the climatological *f(RH)* values for use in the RHR metrics (described in the next section).

The Second IMPROVE Equation (with modifications as detailed in Table 1) is shown in eq 2. It follows a similar form as the First IMPROVE Equation, except the fine mode AS, AN, and OM are split into small ("s") and large ("L") modes with corresponding MSEs and *f(RH)* curves. The fraction of mass in the large mode is the total mass concentration of the species divided by the break point value (20 μg m^{-3}). The large mode mass is the total species mass multiplied by this fraction, and the small mode mass is the total species mass minus the large mode mass (Figure S1a). If the species mass is greater than the break point value, then all mass is assigned to the large mode (Figure S1a). The value of the break point determines whether the small or large mode (and associated MSEs) is weighted more heavily in the reconstruction equation. The equation effectively linearly scales the dry MSE to mass concentrations between 0 and the break point value, using the same break point for AN, AS, and OM (Figure S1b).

$$\begin{aligned} b_{ext} = {} & 2.2 \times f_{SAS}(RH) \times [Small\ Ammonium\ Sulfate] \\ & + 4.8 \times f_{LAS}(RH) \times [Large\ Ammonium\ Sulfate] \\ & + 2.4 \times f_{SAN}(RH) \times [Small\ Ammonium\ Nitrate] \\ & + 5.1 \times f_{LAN}(RH) \times [Large\ Ammonium\ Nitrate] \\ & + 2.8 \times f_{SOM}(RH) \times [Small\ Organic\ Mass] + 6.1 \\ & \times f_{LOM}(RH) \times [Large\ Organic\ Mass] + 10 \\ & \times [Elemental\ Carbon] + 1 \times [Fine\ Soil] + 1.7 \\ & \times f_{SS}(RH) \times [Sea\ Salt] + 0.6 \times [Coarse\ Mass] \\ & + Rayleigh\ Scattering(Site\ Specific) \end{aligned} \quad (2)$$

The modifications included in this equation are similar to those applied in eq 1 (Table 1). The assumptions regarding mass composition include changes to calculations of OM and fine soil. In addition, we used species-specific *f(RH)* curves derived using the same κ values listed above for the large and small size distributions mentioned earlier (Figure 2(b)). These curves (Figure 2(b)) differ from the *f(RH)* curves applied to AS/AN and sea salt reported in Pitchford et al. (2007) and suggested in the 2018 RHR guidance (U.S. EPA, 208; Figure 2(a)). The equation in Pitchford et al. (2007) also included a term for the contribution to light extinction from nitrogen dioxides (NO_2) for sites with measurements. However, we did not include it in eq 1 or 2 here, as it is not routinely used in RHR metrics.

Equations 1 and 2 were both used to calculate total aerosol $b_{ext.}$ However, we used b_{sp} to compare to measurements. The b_{sp} calculations are the same as for b_{ext} but do not include Rayleigh scattering or b_{ext} due to elemental carbon. Additionally, we reduced the contribution of CM by 50% for comparisons based on the nephelometer measurement of coarse b_{sp}, as described in the previous section.

Regional haze rule metrics

A primary purpose for calculating b_{ext} from the speciated mass measurements is to track b_{ext} as an indicator of visibility impairment in CIAs as required by the RHR, while providing some information about the potential sources responsible for the impairment. Thus, considering impacts on RHR impairment calculations is essential to the evaluation of potential updates to the IMPROVE Equation.

Originally, the EPA's guidance on tracking progress on the most anthropogenically impaired days was to calculate haze on each IMPROVE sampling day and track the 5-year annual average of the 20% of days with the highest values (U.S. Environmental Protection Agency 2003). The haze index is measured in deciviews and is calculated from *bext* (eq 3, Gantt et al. 2018; Pitchford and Malm, 1994).

$$Deciview\ Value(dv) = 10 \times ln(b_{ext}/10) \quad (3)$$

Haze can be a product of both natural and anthropogenic sources. Today, wildfire smoke and windblown dust are frequently the source of haziest days at CIAs, especially in the Western U.S.; these are often considered to be natural sources of haze not easily controllable by states. Thus, the RHR guidelines were updated in 2018 with an impairment framework to separate natural haze from anthropogenic impairment (Gantt et al. 2018; U.S. Environmental Protection Agency 2018). The tracking metric is the 5-year annual mean of deciview

values on the 20% most anthropogenically impaired days (MID90) using the Second IMPROVE Equation. The process for calculating the haziest days (days with haze values greater than the 80th percentile per year), clearest days (days in the lowest 20th percentile of haze values per year), and MID90 days (the highest 20th percentile of days ranked by amount of impairment) is outlined in the RHR guidelines (U.S. Environmental Protection Agency 2018).

We calculated RHR metrics with the Second IMPROVE Equation (Table 1) using the assumptions that follow the RHR guidance (U.S. Environmental Protection Agency 2018) as the baseline. The guidelines differ from the assumptions discussed earlier for the modifications to the Second IMPROVE Equation (Table 1). For example, AS is calculated from sulfur (rather than sulfate ion) for the RHR metrics, because it can impact the completion criteria (sulfur and sulfate are determined from different filters). We also followed the RHR guidelines that suggest applying a single *Roc* to calculate OM and calculating fine soil mass following Malm et al. (1994). Fixed site-specific monthly climatological *f(RH)* values are used in the RHR guidelines. While we used climatological values, the *f(RH)* values are species-specific rather than the values currently included in the RHR guidance. These climatological, site-specific *f(RH)* values do not vary annually to avoid changes in calculated trends in visibility being driven by changes in RH. Finally, the RHR metric results include annual completion criteria to be included in the analysis.

Metrics for evaluation

We used several different metrics for evaluation of the agreement between measured ($b_{sp,meas}$) and calculated b_{sp} ($b_{sp,calc}$) to emphasize different parts of the distribution of b_{sp} values, with the number of measurements given as n. Metrics are calculated using daily average values. We reported the Pearson correlation coefficient (r). Following Prenni et al. (2019), we calculated bias as the mean of the differences between calculated and measured b_{sp} (eq 4), and the relative bias as the median of the differences between the calculated and measured b_{sp} divided by $b_{sp,meas}$ (eq 5). We also used the root mean square error (RMSE, eq 6), which gives more weight to the larger errors (at higher concentrations) than the bias and relative bias.

$$Bias = \frac{1}{n}\sum_{i=1}^{n}\left(b_{sp,calc} - b_{sp,meas}\right) \quad (4)$$

$$Relative\ bias = median\left(\frac{b_{sp,calc} - b_{sp,meas}}{b_{sp,meas}}\right)_{i=1}^{n} \quad (5)$$

$$RMSE = \sqrt{\frac{1}{n}\sum_{i=1}^{n}\left(b_{sp,calc} - b_{sp,meas}\right)^2} \quad (6)$$

Results and discussion

We present comparisons of $b_{sp,meas}$ and $b_{sp,calc}$ using the First and Second IMPROVE Equations (eqs 1 and 2, respectively) to understand performance with the most recent nephelometer measurements. We present the trends in MSE assumed when applying the Second IMPROVE Equation to explain the performance of the First and Second IMPROVE Equations. We discuss several analyses designed to understand and adjust for biases described above. Also included is a discussion of attempts to adjust for biases in the Second IMPROVE Equations, primarily by evaluating different break points between the large and small modes. We describe a method to semi-empirically derive new MSEs to apply in a Third IMPROVE Equation, which we then use to compare $b_{sp,meas}$ to $b_{sp,calc}$. Finally, we explore the impacts of a Third IMPROVE Equation on RHR metrics and trends.

Comparison of calculated and measured scattering

Comparisons between b_{sp} measured with the Optec nephelometers and calculated using the First and Second IMPROVE equations (eqs 1 and 2, respectively) are shown in Figure 3 for different time periods (individual site results are shown in Figure S5). Our results differed from Prenni et al. (2019), because we used a greater completeness criterion, stricter filtering to remove poorly calibrated nephelometer data, and a slightly modified Second IMPROVE Equation, and we included data beyond 2016. As discussed in Prenni et al. (2019), the bias increased in the later time periods compared to earlier time periods (also shown in Figure S6). However, unlike Prenni et al. (2019), we found little change in correlation across time periods.

For both equations, the relative bias was greatest and most variable at the lowest b_{sp} values (Figures 3 and S7), consistent with the expected uncertainty of the Optec nephelometer measurements, which is approximately 100–200% at 1–2 Mm^{-1} (Molenar 1997, 2000). As b_{sp} increases, the measurement uncertainty decreases, and correspondingly, Figures 3 and S7 indicate reduced relative bias and variability in the comparison between measured and calculated b_{sp} across all time periods. When applying the First IMPROVE Equation, however, the reduction in relative bias with increasing b_{sp} was accompanied by a transition from positive to negative bias, such that measured b_{sp} was underpredicted at

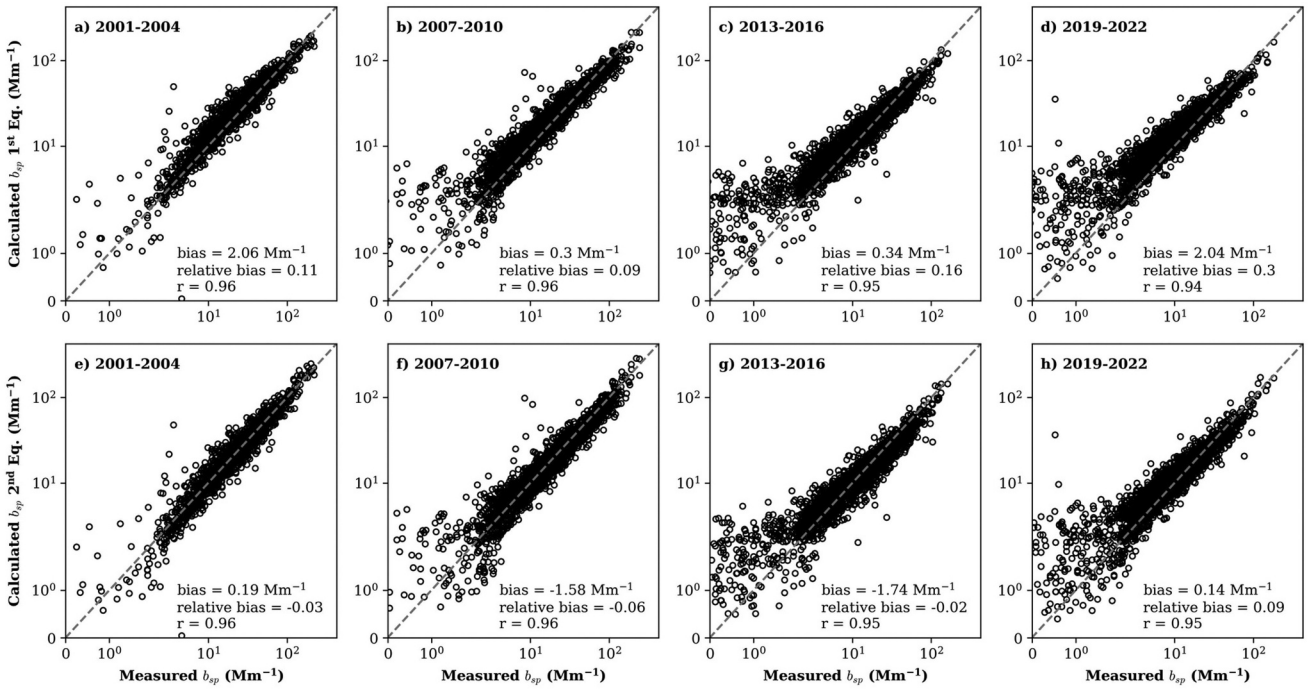

Figure 3. Scatter plots of ambient aerosol scattering (b_{sp}, Mm^{-1}, 550 nm) calculated using the First IMPROVE Equation (top row, "1st eq") and Second IMPROVE Equation (bottom row, "2nd eq") vs. b_{sp} measured by Optec nephelometers for the following years: 2001–2004 (panels a, e), 2007–2010 (b, f), 2013–2016 (c, g), and 2019–2022 (d, h). The dashed line shows the 1:1 line, and statistics for the given time period are provided in each panel. IMPROVE sites used for the analysis are shown in Figure 3.

higher values and overpredicted at lower values. The Second IMPROVE Equation (Pitchford et al. 2007) was developed to address this systematic bias, and for 2001–2004, it did reduce the bias. However, as shown in Figure 3, a similar bias pattern (low bias at high concentrations and high bias at low concentrations) persisted after the early years of 2001–2004, even when using the Second IMPROVE Equation (also shown in Figure S7).

Comparisons between calculated b_{sp} and b_{sp} measured using data from the 2-WIN nephelometers are more limited, as installation only began in 2022 (Table S1 gives the periods of data available for each 2-WIN site). The comparison between measured and calculated b_{sp} with the First IMPROVE Equation (Figure 4(a)) and Second IMPROVE Equation (Figure 4(b)) uses all available 2-WIN data through 2024. The comparisons for individual sites are provided in Figure S8.

Using the first equation for the comparison with the 2-WIN dataset (Figure 4(a)) leads to a positive bias at low b_{sp} values (in the range of ~1–10 Mm^{-1}) and a negative bias at high b_{sp} values (~100 Mm^{-1}). While this trend in the bias is less evident when using the second equation (Figure 4(b)), the calculated b_{sp} has a greater negative bias and relative bias compared to the calculated b_{sp} using the First IMPROVE Equation. The negative bias in calculated b_{sp}, using both equations, is greater for the 2-WIN dataset compared to results using the Optec dataset. However, the biases at low and high b_{sp} values can have important implications for RHR metrics, which track trends in the clearest and most anthropogenically impaired days. Thus, we further evaluated this bias by comparing measured and calculated b_{sp} on the days that are categorized as clearest and MID90 days following the RHR guidelines.

The statistics for the comparison on the clearest and MID90 days are given in Table 2. The full time period for the Optec dataset is used to show the impact in reference to the long-term trends in the RHR; separating into the time periods, as in Figure 3, would provide different results. Based on the previous analysis, a positive bias is expected on the clearest days and a negative bias on the MID90 days. Additionally, based on the impetus for the second equation, using the Second IMPROVE Equation should have less bias than using the First IMPROVE Equation for both the clearest and MID90 days. For the clearest days, using the Second IMPROVE Equation reduced the bias in $b_{sp,calc}$ compared to the Optec nephelometer measurements. However, for the 2-WIN dataset, using the Second IMPROVE Equation leads to an underestimation in $b_{sp,calc}$ on the clearest days. For the MID90 days, using the Second IMPROVE Equation makes the comparison, in terms of bias and RMSE, worse for both the Optec

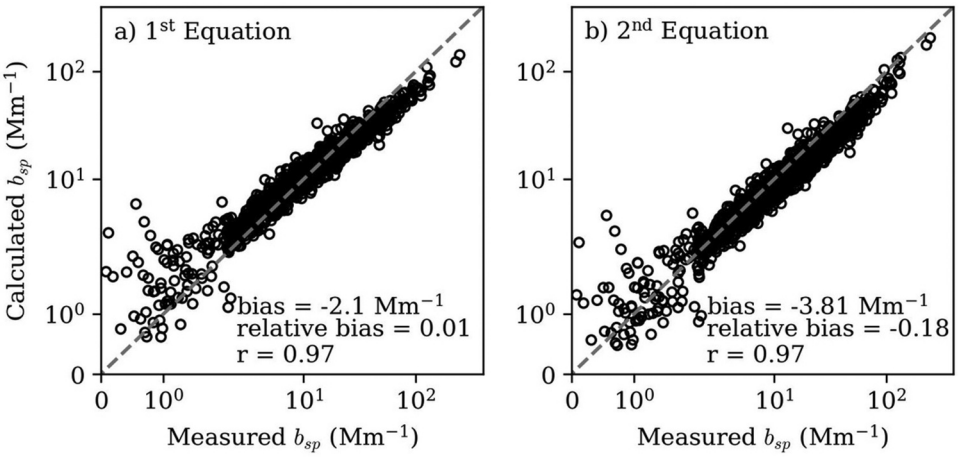

Figure 4. Scatter plots of ambient aerosol scattering (b_{sp}, Mm^{-1}, 550 nm) calculated using the (a) First IMPROVE Equation and (b) Second IMPROVE Equation and measured by 2-WIN nephelometers for all available data in 2022–2024 (Table S1). The gray dashed lines are the 1:1, and statistics for the given time period are provided in each panel. IMPROVE sites used for the analysis are shown in Figure 1.

Table 2. Statistics (bias, relative bias, RMSE) for comparison between measured (using the Optec or 2-WIN dataset) and calculated b_{sp} (using the First and Second IMPROVE Equations) on days designated as clearest days or MID90 days in the RHR calculations (using the first or second equation).

		Clearest days					MID90 days				
Equation	Neph. and time period	Mean calc. dv	b_{sp} bias (Mm^{-1})	b_{sp} Rel. bias	b_{sp} RMSE (Mm^{-1})	# Site-days	Mean calc. dv	b_{sp} Bias (Mm^{-1})	b_{sp} Rel. bias	b_{sp} RMSE (Mm^{-1})	# Site-days
1st eq	Optec, 2001–2022	7.0	1.5	0.29	4.1	2042	15.0	−0.3157	0.09	10.1	2146
2nd eq	Optec, 2001–2022	6.6	0.16	0.07	4.4	2038	14.3	−2.0	−0.04	10.4	2162
1st eq	2-WIN, 2022–24	6.0	0.53	0.14	1.1	267	14.4	−4.0	−0.12	8.0	309
2nd eq	2-WIN, 2022–2024	5.3	−0.47	−0.10	1.2	265	13.6	−6.3	−0.27	9.1	307

The average calculated total visibility ("mean calc. dv") using the mass concentrations and the specific equation on designated clearest and MID90 days, which also correspond to nephelometer measurement days, is also given. The number of days changes between equations due to slightly different days selected as most impaired or clearest, which may or may not have valid nephelometer measurements.

and 2-WIN datasets. This suggests that using the Second IMPROVE Equation further underestimates visibility impairment on the MID90 days. Thus, in terms of representing b_{sp} on days pertinent to the RHR metrics, the Second IMPROVE Equation is not a clear improvement over the First IMPROVE Equation.

Trends in mass scattering efficiencies used in the Second IMPROVE Equation

As in Prenni et al. (2019), we showed that using the Second IMPROVE Equation led to poorer agreement between measured and calculated b_{sp} over time. In Prenni et al. (2019), this was attributed to the break point value used to apportion mass between the large and small modes. The break point was empirically derived using mass concentrations from the early 2000s, but strong decreases in AS mass concentrations across the U.S. have occurred since (Figure 5(a)). The trend in the average (of both modes) dry MSEs for AS, AN, and OM determined using the Second IMPROVE Equation across years (for all sites with Optec nephelometers) is shown in Figure 5(b) and emphasizes that the scaling of MSE with mass in the Second IMPROVE Equation results in strong declines in derived MSEs over time (Figure 5(b) and Figure S9).

It is evident from Figure 5(b) that the average MSEs used in the Second IMPROVE Equation are much lower than the MSEs in the First IMPROVE Equation, shown as the constant dashed lines for OM (4 m^{2}g^{-1}) and AS and AN (3 m^{2}g^{-1}), as also noted in Lowenthal and Kumar (2016). In 2001–2004, using the First IMPROVE Equation overpredicted scattering compared to measurements (Figure 3(a)), and using the lower MSEs in the Second IMPROVE Equation reduced the bias (Figure 3(e)). However, AS mass concentrations declined after this early period, particularly in the Eastern U.S. (Figure S9). By coupling MSEs to mass concentrations in the Second IMPROVE Equation, there is also an assumed lowering of derived dry MSE values (Figure 5(b), annual median of 2.5 m^{2}g^{-1} in 2001 to 2.3 m^{2}g^{-1} in 2022 for all Optec sites). As b_{sp} is calculated as a multiplication of mass

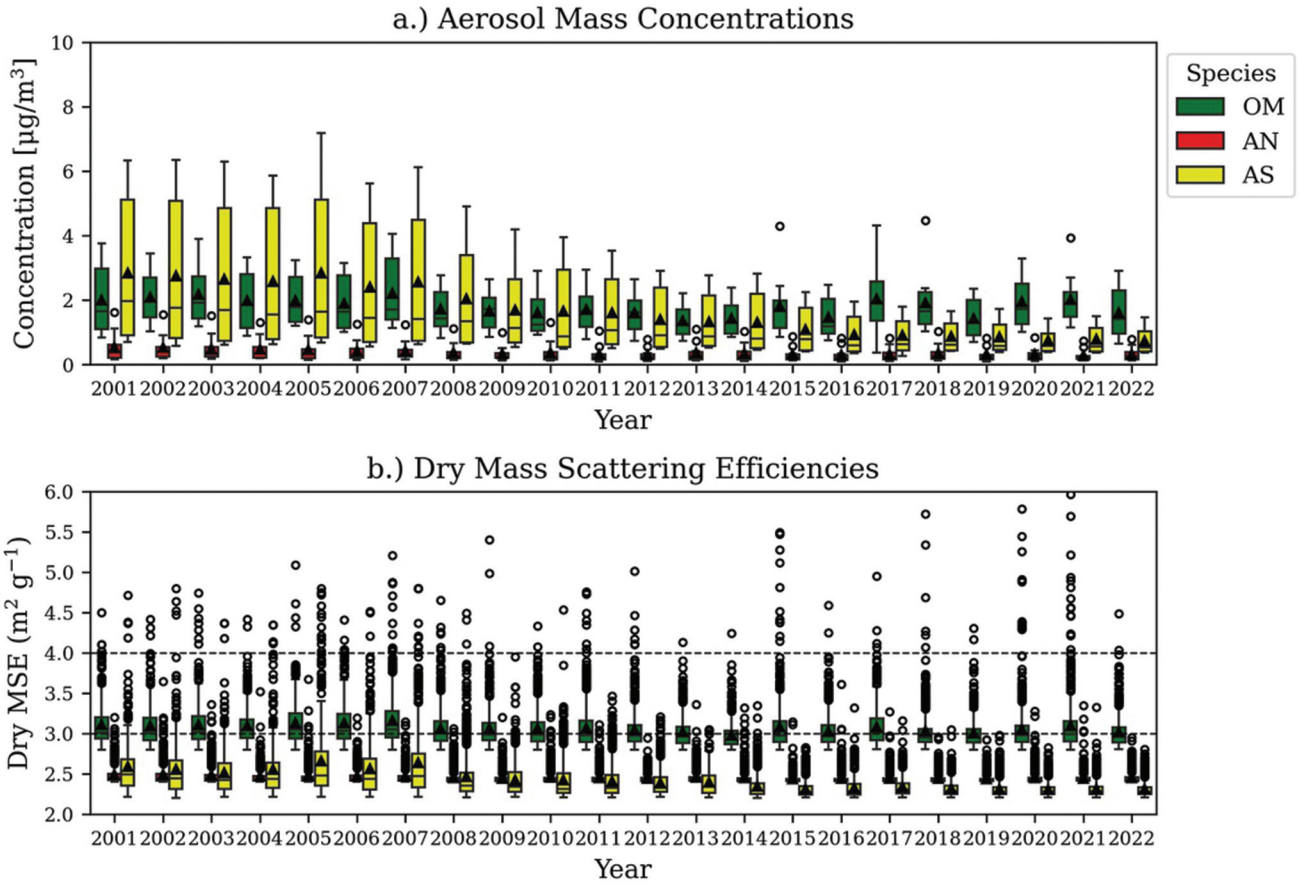

Figure 5. (a) Distribution of annual average concentrations of organic matter (OM, green), ammonium sulfate (AS, yellow), and ammonium nitrate (AN, red) across all IMPROVE sites with Optec nephelometers shown in Figure 1 and (b) annual distribution of average (of both modes) dry mass scattering efficiencies (m^2g^{-1}) OM, AS, and AN used with the Second IMPROVE Equation for all daily measurements in a year across the same sites. Dashed lines in (b) represent the constant dry MSE values used in the First IMPROVE Equation for OM (4 m^2g^{-1}) and AS and AN (3 m^2g^{-1}). The box shows the quartiles of the dataset, while the whiskers extend to 1.5 interquartile range, and outliers are shown as open circles. Black triangles denote the means of the distribution.

concentration and MSE, this coupling leads to steeper decreasing trends in calculated b_{sp} over time, compared to using fixed MSE values. As noted in Prenni et al. (2019), decreases in average MSE values determined with the Second IMPROVE Equation are not likely representative of actual changes in MSE in the atmosphere, and aerosol size distributions have not shown a corresponding shift to smaller particles with decreasing mass concentrations.

The apportionment between the small and large modes (less efficient and more efficient scattering, respectively) is determined by the break point. Because the break point is too high relative to current mass concentrations, Lowenthal and Kumar (2016) suggested simply lowering it to apportion more mass to the large mode and thereby increase MSEs. Prenni et al. (2019) suggested that the break point needed to vary by site and over time, and ideally for each species, to avoid biases in calculated b_{sp} using the split-component model. In the following section, we present results testing methods for adjusting the break point.

Adjusting the break point between large and small mode particles for the Second IMPROVE Equation

In the Second IMPROVE Equation, the break point is used to apportion mass between the $PM_{2.5}$ small and large modes based on the assumption that higher concentrations correspond to aging and growth of particles. The current break point of 20 µg m^{-3} and the lower mass concentrations of recent years result in most of the mass being apportioned to the small mode, which implies that there is significantly less aging of aerosol particles in the current environment. While changes in emissions and atmospheric conditions could alter pathways, aerosol aging still occurs, and there should not be

an elimination of the large mode. Prenni et al. (2019) showed that the decreases in mass concentrations at GRSM1 were not associated with shifts in aerosol size distributions. Thus, while MSE values may follow the general form used in the Second IMPROVE equation (Figure S1), the equation should be modified to allow representation of aerosol aging, even at low mass concentrations. Lowering the break point would allow for the representation of aerosol aging and the presence of large-mode aerosols at lower concentrations.

In this section, we explore altering the break point used in the Second IMPROVE Equation using several different methods to minimize the difference (in bias, relative bias, or RMSE) between measured and calculated b_{sp}. This is to test the feasibility of systematically altering break points, and thus the mass in the small and large modes. For this analysis, the assumed size distribution of each mode and associated MSEs and *f(RH)* of each of the two modes was not changed.

The results of determining the optimal break points using the Optec dataset are shown in Figure 6. The values in this figure are the single (i.e., same for all three species) break points that would lead to the minimal difference (defined using the lowest RMSE) between measured and calculated b_{sp} for each year at each site. Results using relative bias as the optimization parameter are shown in Figure S10. Results from this process showed some agreement with the method in Prenni et al. (2019), in that for many sites the optimal break point decreased over time to much less than 20 μg m^{-3}. This was not true for all sites; in fact, optimized break points greater than 20 μg m^{-3} at some sites (e.g., GRCA2, GLAC1) suggest that the current derived MSEs are too high, leading to overpredictions in calculated b_{sp}. However, there are several issues with the assumptions used in this optimization approach. One, we used the same break point for all species. Additionally, using a shorter or longer timescale than a year in the optimization produced different results. An additional error is introduced as different years have different numbers of valid observations. Finally, while some of the results appear to be logical (i.e., following a downward trend over time), there are site-years where the optimal break point was unrealistically high. And finally, as Figure S10 shows, the results can vary depending on the metric used for optimization (e.g., GRCA2). The resulting optimal break points were also not directly correlated with mass concentrations at a site; thus, determining the optimal break point would require having the mass and optical measurements at every site for the year. This is not a feasible endeavor and puts increasing emphasis on the nephelometer measurements over the mass measurements.

The "optimal" break point for all sites and time periods in the Optec dataset was determined to be 12 μg m^{-3} (using the lowest RMSE). Over 2001–2022, using this break point reduced the bias compared to the First or Second IMPROVE Equations (Table 2), but it performs worse in shorter time periods: higher break points fit earlier years better, while lower break points fit later years better due to declining mass concentrations. A 12 μg m^{-3} break point produces a higher early-period bias and shifts the bias trend forward in time. Comparisons with 2-WIN nephelometer b_{sp} data show

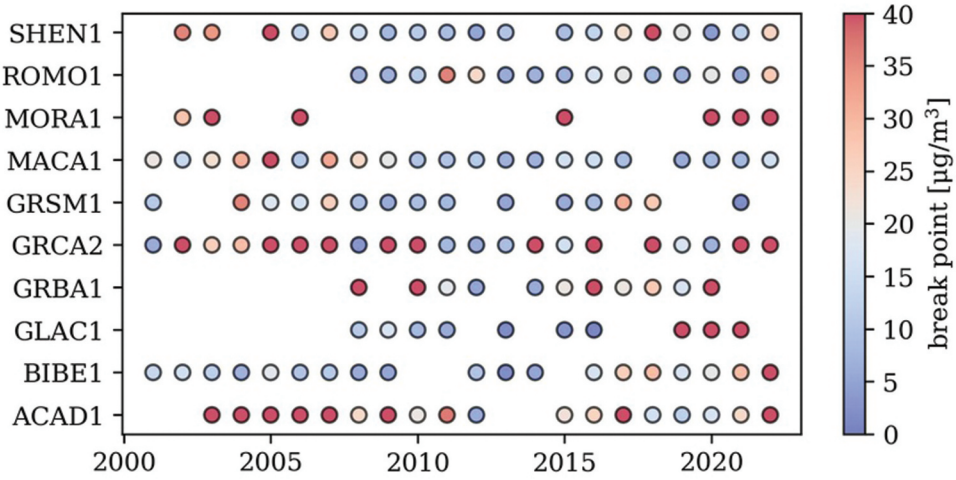

Figure 6. Mass break point (μg m^{-3}) used to apportion large and small mode fractions for the Second IMPROVE Equation corresponding to the lowest RMSE between calculated and measured b_{sp} for each site and each year in the Optec dataset. The current break point is 20 μg m^{-3}; thus, blue colors suggest a lower break point corresponds to better agreement, while red points suggest a larger break point corresponds to better agreement. Note that this analysis uses the same break point for organic matter, ammonium sulfate, and ammonium nitrate.

slight improvements in terms of bias and relative bias with this lower break point, though the results are not better than using the First IMPROVE Equation.

We also tested the Prenni et al. (2019) method, which sets the break point annually for each site and species as five times the median concentration. This approach, in general, lowers the break point over time and increases the average mean dry MSE relative to the Second IMPROVE Equation (Figure 6), yielding average values of 2.8 m^2 g^{-1} for AS, 3.2 m^2 g^{-1} for AN, and 3.7 m^2 g^{-1} for OM for data from the sites and time periods included in both the Optec and 2-WIN datasets. This method does not provide better agreement with the Optec measurements compared to using the First IMPROVE Equation (Table 3) and suggests that the break points determined in this method may be too low, leading to dry MSE values that are too high for some or all species. Using a higher multiplier of the median annual concentration does reduce the bias for some of the time periods; however, this fact further emphasizes that, across the network, the break point is not directly or consistently related to mass concentrations over time. With the 2-WIN dataset, the Prenni et al. (2019) method does reduce the bias and relative bias for the full dataset. However, when comparing for the individual sites (not shown), the method improves the comparison between calculated and measured b_{sp} at less than half the sites (in terms of relative bias and/or bias), which again emphasizes that the method does not perform consistently.

This analysis suggests that an optimized version of the Second IMPROVE Equation could provide better agreement with $b_{sp,meas}$ from either nephelometer dataset. However, the optimization would be best done for different time periods and on a site-by-site basis. This endeavor would be a data optimization that is not directly tied to trends in mass concentrations and thus creates additional uncertainties for sites without co-located nephelometers. The First IMPROVE Equation has proven to be more consistent with the changing aerosol concentrations and composition over time. Consequently, in the next analysis, the First IMPROVE Equation is optimized by updating the MSEs.

Deriving mass scattering efficiencies for the First IMPROVE Equation

There are multiple ways to derive MSEs, as discussed in Hand and Malm (2007), such as from theoretical calculations, measurements, or multiple linear regression (MLR). The methodology, in addition to the physiochemical differences in the aerosols, can lead to variability in the results. In this work, two methods were used: (1) MLR, and (2) a minimization using sets of values determined from modeled size distributions and Mie theory. A description of the MLR method (which follows Hand and Malm 2007) and results are discussed in the supplement. Using MLR on different time periods suggested different regression coefficients (Figure S11), but for the full time series of the Optec data, the regression coefficients were generally equivalent to the MSE already used in the First IMPROVE Equation (Table S3; 3.0, 3.0, 4.0 m^2g^{-1} for AS, AN, and OM, respectively). However, to perform the regression, we held the *f(RH)* curves constant for each species. Thus, while the regression coefficients may be interpreted as MSE, they may also include biases in other assumptions, like *f(RH)*. Thus, we instead used a semi-theoretical approach to evaluate MSEs. We calculated lognormal monomodal size distributions over a range of *Dp* (0.2 to 0.5 µm) and σ_g (1.5–2.2). Dry MSE and $b_{sp,dry}$ were calculated for each size distribution using Mie theory and refractive indices and density values of 1.53 and 1.77 g cm^{-3} for AS, 1.55 and 1.73 g cm^{-3} for AN, and 1.55 and 1.4 g cm^{-3} for OM. The *f(RH)* curves (Table S3) were determined by "growing" the dry size distribution using diameter growth curves (*D/Do*, Table S4) to

Table 3. Biases for comparison between measured b_{sp} by Optec or 2-WIN nephelometers and calculated b_{sp} using the First IMPROVE Equation, Second IMPROVE Equation with a break point (bpt) of 20 µg m^{-3}, the Second IMPROVE Equation with a break point of 12 µg m^{-3} for different time periods, and the Second IMPROVE Equation with varying break points as in Prenni et al. (2019, "P2019").

	Years	Metric	1st eq	2nd eq, bpt = 20	2nd eq, bpt = 12	2nd eq, P2019
Optec Nephelometers	2001–2004	Bias [Mm^{-1}]	2.06	0.19	2.64	3.24
		Rel. Bias	0.11	−0.03	0.03	0.08
	2007–2010	Bias [Mm^{-1}]	0.30	−1.58	0.40	1.47
		Rel. Bias	0.09	−0.06	−0.01	0.07
	2013–2016	Bias [Mm^{-1}]	0.34	−1.74	−0.90	1.3
		Rel. Bias	0.16	−0.02	0.01	0.16
	2019–2022	Bias [Mm^{-1}]	2.04	0.14	0.91	3.46
		Rel. Bias	0.30	0.09	0.12	0.31
	2001–2022	Bias [Mm^{-1}]	1.23	−0.70	0.78	2.46
		Rel. Bias	0.17	0.00	0.05	0.17
2-WIN	2022–2024	Bias [Mm^{-1}]	−2.10	−3.81	−2.83	−0.43
		Rel. Bias	0.01	−0.18	−0.15	−0.01

calculate $b_{sp,RH}$ for a range of RH values (0–100%). D/Do curves were obtained using κ values of 0.61, 0.67, and 0.1 for AS, AN, and OM, respectively. The corresponding MSEs and *f(RH)* are shown in Figure S12.

The MSE and *f(RH)* curves for each size distribution were used to calculate $b_{sp,calc}$ values (assuming AS, AN, and OM have the same size distribution), which were then evaluated against $b_{sp,meas}$ to determine the optimal size distribution (and MSE) resulting in the best agreement. Results were evaluated using bias, relative bias, and RMSE (eqs 4-6) (Figure S13). Data from the 2-WIN, the full Optec dataset, and a subset of the Optec data covering the two later periods of analysis in Figure 4 (i.e., the last decade of Optec measurements, 2013–2022) were tested separately. Each of these datasets resulted in slightly different optimal size distributions (Figure S13). For example, minimizing the relative bias for the full Optec data suggested that the size distribution with the lowest *Dp* (0.2 µm, σ_g of 1.7–2.1) should be used, while using the 2-WIN data suggested that the current *Dp* of 0.3 µm (σ_g of 2.2) works well. If optimizing based on bias, which emphasizes the higher b_{sp} values, the optimal size distribution was shifted to those with slightly larger *Dp* for both datasets. Results suggest that the optimal size distribution also varied by site. As there was not a single optimal size distribution for both the Optec and 2-WIN datasets, we selected a size distribution that resulted in low relative bias for the 2-WIN dataset and a low bias for the Optec dataset (different statistics were used because of the smaller sample set for 2-WIN). Thus, we suggest using a *Dp* of 0.3 µm with a σ_g of 2.2. This size distribution corresponds to dry MSEs of 3.0 m^2g^{-1} for AS, 3.2 m^2g^{-1} for AN, and 4.0 m^2g^{-1} for OM. These MSEs are very similar to the values in the First IMPROVE Equation, are broadly consistent with the results using MLR (Table S3), and correspond to consistent *f(RH)* curves for each species (Table S4).

Final comparisons and recommendations for a new IMPROVE equation

The Second IMPROVE Equation did not perform better than the first equation consistently over time due to the equation shifting too much of the mass to the small mode, resulting in lower average MSE values. As there is not a clear method to alter the break point to allow for the representation of aerosol aging with declining mass, we recommend returning to the form of the First IMPROVE Equation, but with several modifications. In addition to the modifications to the underlying mass calculations (increased dust concentrations and a monthly-varying *Roc*), the inclusion of b_{sp} from sea salt (with an updated $f_{SS}(RH)$), and the addition of an *f(RH)* curve for OM as in the First IMPROVE Equation (eq 1); we also suggest using dry MSEs that correspond to a single aerosol size distribution (3.0, 3.2, and 4.0 m^2g^{-1} for AS, AN, and OM, respectively) and corresponding species-specific *f(RH)* curves for AS, AN, and OM (Table S3). The new equation, referred to here as the "Third IMPROVE Equation," is given in eq 7. For completeness, the contribution from NO_2 should be added ($0.33 \times [NO_2]$), though we do not include it, as this term is not routinely included in RHR calculations.

$$\begin{aligned} b_{ext} = {} & 3.0 \times f_{AS}(RH) \times [Ammonium\ Sulfate] \\ & + 3.2 \times f_{AN}(RH) \times [Ammonium\ Nitrate] \\ & + 4.0 \times f_{OM}(RH) \times [Organic\ Mass] \\ & + 10 \times [Elemental\ Carbon] + 1 \times [Fine\ Soil] \\ & + 0.6 \times [Coarse\ Mass] + 1.7 \times f_{SS}(RH) \times [Sea\ Salt] \\ & + Rayleigh\ scattering(Site\ Specific) \end{aligned} \tag{7}$$

The comparisons for the Optec and 2-WIN data compared to the $b_{sp,calc}$ using the Third IMPROVE Equation are presented in Figure 7. Because the MSEs and *f(RH)* curves are similar to the First IMPROVE Equation, the statistics are almost identical to earlier comparisons with the First IMPROVE Equation. The similarity of the Third IMPROVE Equation to the First IMPROVE equation illustrates the robustness of the original equation.

Figure 7 demonstrates that the bias between measured and calculated $b_{sp,}$ has not been completely removed, nor has the variability in bias over time. These results emphasize that a single semi-empirical equation will not be able to represent the varying aerosol properties across all sites and all times. Developing an appropriate equation for a specific location would require nephelometer measurements, mass composition measurements, and measurements of size distributions. However, the goal here is to promote an equation best suited for tracking visibility over time and network wide. The Third IMPROVE Equation uses the most up-to-date representations of species mass (Hand et al. 2019, 2024); provides more consistent results across the different time periods, sites, and datasets; and should minimize potential biases in the RHR metrics over time.

Impact on most anthropogenically impaired days and regional haze rule trends

In this section, the impact of using the Third IMPROVE Equation on the RHR metrics (Clearest Days, MID90) is

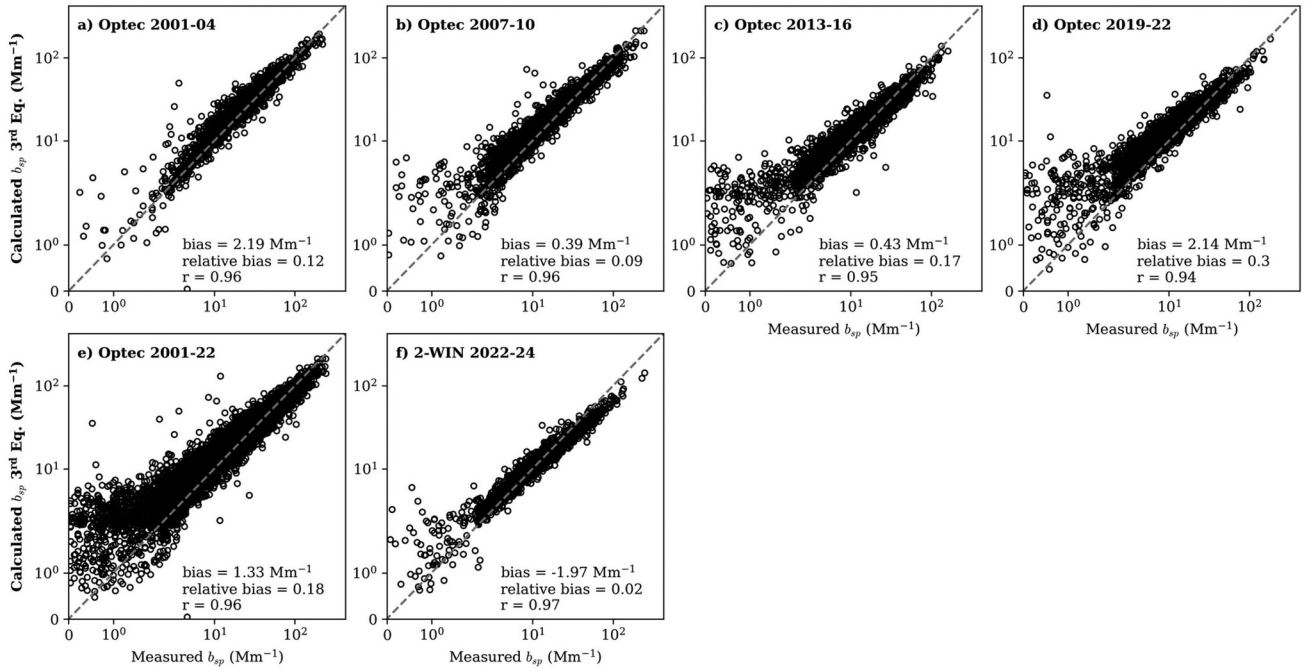

Figure 7. Scatter plots of ambient aerosol scattering ($b_{2806″ =″0″>sp}$) calculated using the Third IMPROVE Equation with new dry MSEs and *f(RH)* curves for OM, AS, and AN; (a-d) comparisons for Optec nephelometers in different time periods, as in Figure 2, (e) comparison for all of the Optec data, and (f) comparison for the 2-WIN data (scattering from CM was not included). Dashed lines are the 1:1, and statistics for the given time period are provided in each panel. IMPROVE sites used for the analysis are shown in Figure 1. Values correspond to a wavelength of 550 nm.

shown. As discussed in the Methods, the "MID90" is the annual average dv of the 20% most anthropogenically impaired days (days with more anthropogenic pollution as opposed to smoke or dust), as determined using the speciated mass concentrations. Results are compared to values determined using the version of the Second IMPROVE Equation in the RHR guidance (U.S. Environmental Protection Agency 2018). For the Third IMPROVE equation, climatological *f(RH)* values were approximated by scaling the current RHR climatological *f(RH)* to account for the difference in the size distributions used. Sensitivity testing showed that this scaling method may introduce a small error of less than 10% in the *f(RH)* values. Trends in the annual MID90 and clearest days using the different equations at the same Optec sites are shown in Figure 8.

Sites in the Eastern U.S. (SHEN1, MACA1, ACAD1, GRSM1) had higher MID90 dv values in the 2000–2004 time period, with values decreasing in the later time periods (this trend is corroborated by the measured b_{sp} values on the corresponding MID90 days, Figure S13). Because the second equation gives higher b_{sp} values at high concentrations and lower values at low concentrations (relative to the third equation, Figure S14), it produces a steeper impairment trend at these sites than using the Third IMPROVE Equation, consistent with overestimating progress as discussed previously. Using the Third IMPROVE equation reduces the magnitude of the trend, driven primarily by changes to the MSE for AS (Figure S15). Most impaired days at sites in the Western U.S. (ROMO1, MORA1, GRCA2, GRBA1, GLAC1) had lower MID90 dv values during the entire time period, and thus, there is only a slight increase in MID90 dv values across the whole time period when using the Third IMPROVE equation. While the Third IMPROVE Equation includes updates that enhance scattering—such as increased dust and water uptake by organics—the primary driver of the changes is the use of higher MSEs compared to those used in the second equation (Figure S16). Considering differences across all IMPROVE RHR sites (not just the sites in Figure 8), we find that the Third IMPROVE Equation increases the calculated dv values on the most anthropogenically impaired days and on the clearest days (Figure 9) compared to the Second IMPROVE equation applied in the RHR guidance (U.S. Environmental Protection Agency 2018, Table 1). In the earlier period (before 2010), MID90 dv values show a wider range of differences in dv between the two equations, with some sites exhibiting decreases in MID90 dv values when using the Third IMPROVE Equation. However, by the later time periods, lower values of dv are calculated with the Third Equation for very few sites, a pattern consistent with the site-level comparisons in Figure 8. The differences between using the two equations are ~1–2 dv for MID90 values for all

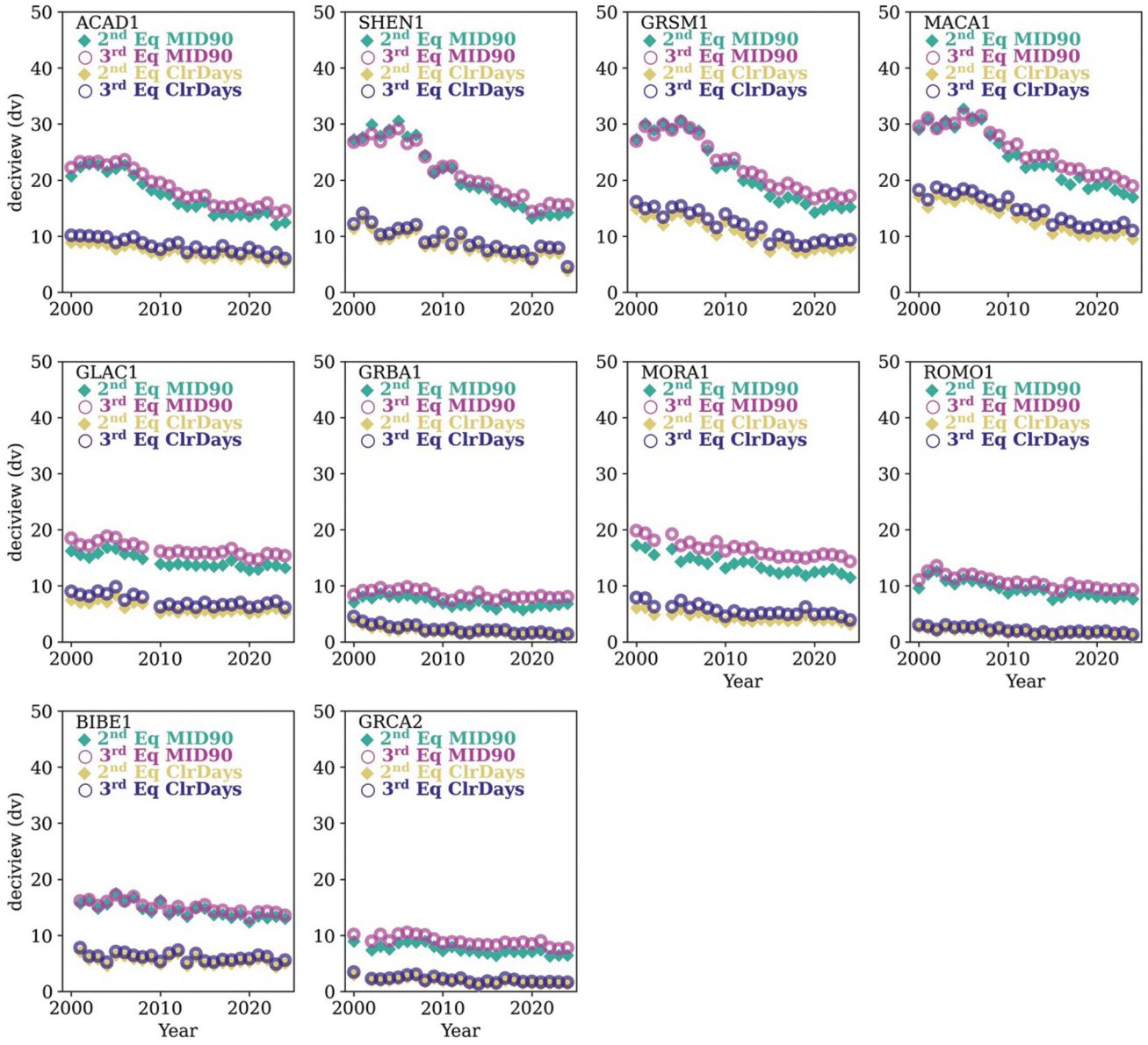

Figure 8. Annual average values of haze index (dv) for 2000–2024 on the most anthropogenically impaired days (MID90) and clearest days (ClrDays) at select IMPROVE sites using the Second IMPROVE Equation as in the RHR guidance (Table 1) and Third IMPROVE Equation.

sites and ~0.5–1 dv on the clearest days. As b_{sp} and MID90 dv values have been decreasing across the network (e.g., Figure S13), this change becomes more important. Additionally, while the "2064 Endpoints" are calculated from the "natural conditions" on the MID90 days, our clearest days comparison suggests that our changes to the equation would increase these values.

Conclusion and recommendation

We evaluated the performance of the IMPROVE reconstructed b_{ext} equations by comparing measured and calculated b_{sp} at IMPROVE sites with co-located nephelometers across the U.S. This study is a continuation of past analyses to evaluate and refine the IMPROVE reconstructed b_{ext} equation used to track haze trends in the RHR. The analyses included comparisons of data from Optec nephelometers from 2001–2022 and data from the recently deployed 2-WIN nephelometers (2022–2024). Our results, which included more rigorous quality assurance and removal of more suspect Optec data than in past analyses, suggested that some of the previously reported trends in disagreement between measured and calculated b_{sp} over time were due to instrument degradation and periods of poor calibration for the Optec nephelometers. Data

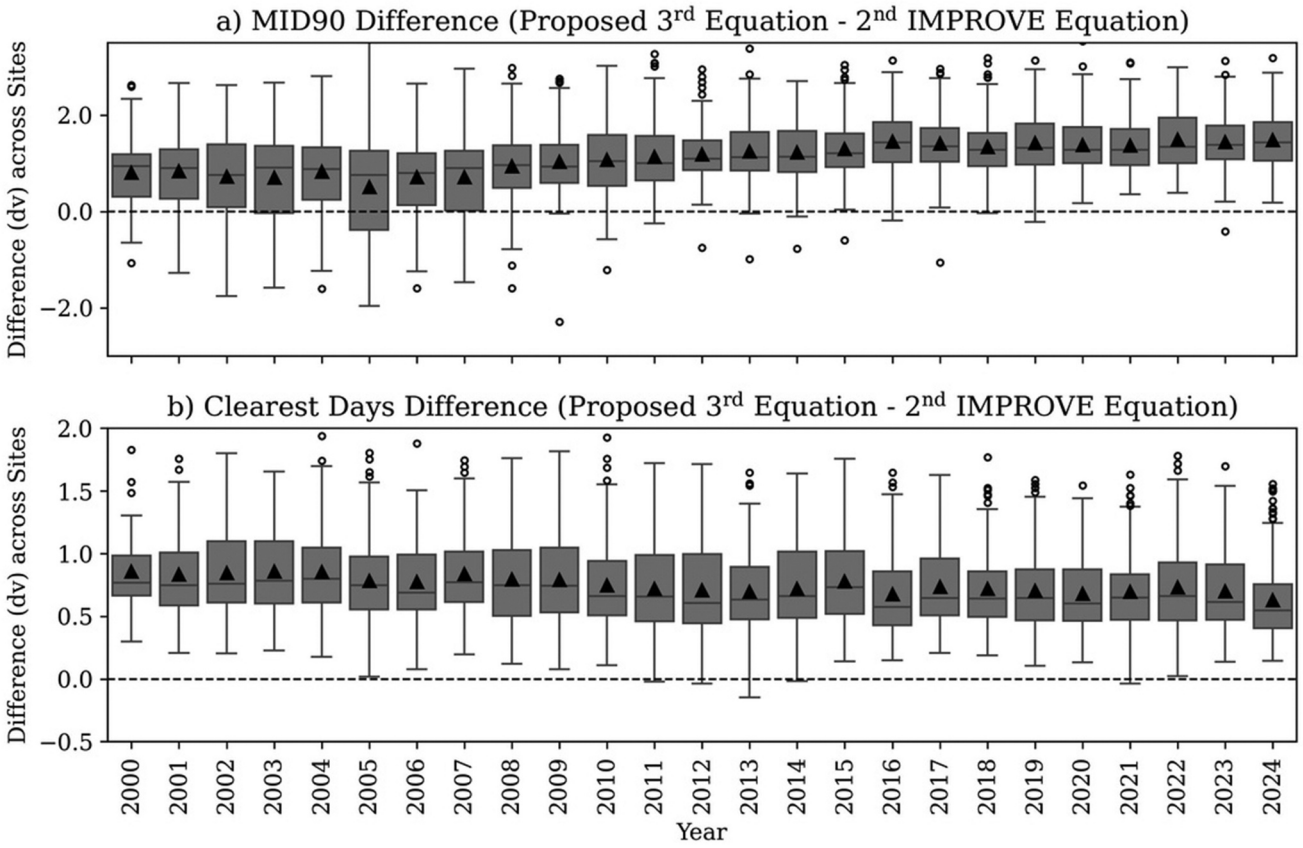

Figure 9. Box plots of the distribution across all 110 IMPROVE RHR sites of the difference between the annual (a) MID90 and (b) clearest day deciview values using the Third IMPROVE Equation and the Second IMPROVE Equation (as currently used in the RHR guideline, Table 1) for each year. The box shows the quartiles of the dataset, while the whiskers extend to 1.5 interquartile range, and outliers are shown as open circles.

from the 2-WIN nephelometers showed better agreement between $b_{sp,meas}$ and $b_{sp,calc}$ for recent time periods.

The Second IMPROVE Equation was developed to correct the tendency of the First IMPROVE Equation $b_{sp,calc}$ to overpredict at low b_{sp} values and underpredict at high values. The formulation of the Second IMPROVE Equation assumes that at low aerosol mass concentrations, most of the aerosol mass is in the small mode, with less efficient scattering. At higher mass concentrations, more aerosol mass is in the large mode, with more efficient scattering. To represent this assumption, MSEs are interpolated between small-mode and large-mode MSE values as a function of aerosol mass concentration, with the interpolation controlled by a fixed break point that defines the transition between the modes. As several previous studies have suggested, there is some statistical relationship between mass concentration and MSE; however, the current break point was empirically fit for early measurements when concentrations were, on average, higher, particularly in the Eastern U.S. The comparison of $b_{sp,calc}$ and $b_{sp,meas}$ showed that using the Second IMPROVE Equation reduced the overprediction of $b_{sp,calc}$ at low b_{sp} values and the underestimation at high b_{sp} values in the earliest Optec years, specifically for the Eastern U.S. sites (Figures 4, 5, S6). However, as mass concentrations decreased, the split-component equation assigned increasingly more of the aerosol mass to the small mode with less efficient scattering over time, an assumption not reflected in aerosol size distribution measurements (Prenni et al. 2019). Our results showed that for the full time period of the Optec data, and for the recent 2-WIN data, the Second IMPROVE Equation does not clearly provide an advantage.

As the break point in the Second IMPROVE Equation is, in general, too high for current aerosol mass concentrations, we tested varying the break point between small- and large-mode aerosols with mixed results. While the break point between small and large modes can be optimized, for best results, the break point needs to be varied over time and be site-specific. Thus, if the goal of a future study is to best match observations at a site, a modified version of the Second IMPROVE Equation with a site-specific break point may be

appropriate. However, in our analysis, the optimal break point was not strictly correlated with mass concentrations. Thus, it would be difficult to determine optimal break points for sites without corresponding nephelometer measurements. Additionally, the process would be arduous to implement in the RHR and in modeling efforts, and possibly introduce more bias into the visibility trend analysis.

Early RHR guidance focused on tracking trends on the haziest days (U.S. EPA 1999, 2003); thus, it was imperative to reduce any bias at high values and was the impetus for developing the Second IMPROVE Equation. The shift to the most anthropogenically impaired framework in the current RHR guidelines (U.S. EPA 2018) leads to less emphasis on the days with the highest b_{ext} values, which are now often due to smoke or dust, and instead tracks trends for most anthropogenically impaired days, which have b_{ext} values that are more in the middle of the scattering distribution. The First IMPROVE Equation performs better and more consistently in this range (i.e., Figure S6). Thus, for tracking trends for the RHR, we suggest returning to a modified form of the First IMPROVE Equation. As suggested in previous work (Prenni et al. 2019), an update to the equation should also address biases in the calculated mass concentrations, *Roc*, and OM hygroscopicity. We therefore introduced the Third IMPROVE Equation (eq 7) for consideration for use in the RHR. This equation includes the following updates:

(1) It uses the updated equation for estimating dust mass concentrations, as in Hand et al. (2019).
(2) It uses a monthly-varying *Roc* for estimating OM mass concentrations, as in Hand (2019, 2024).
(3) It assumes a single size distribution that does not vary with concentration (mean diameter of 300 nm with a geometric standard deviation of 2.2) for AS, AN, and OM, and uses the corresponding MSE values for each species (3, 3.2, and 4 m^2g^{-1}; respectively).
(4) It uses species-specific *f(RH)* curves that correspond to the assumed size distribution of OM, AS, AN, and SS (given in Table S3).

If this IMPROVE equation is adopted for the RHR, then new climatological *f(RH)* values should be derived based on the assumed particle size distributions. Biases will still occur when using the Third IMPROVE Equation for comparing calculated to measured b_{sp} values because it is a general equation applied to specific sites under varying aerosol conditions. However, this equation better aligns with conclusions from recent IMPROVE studies, reflects the latest scientific research, is consistent in assumptions regarding aerosol size distributions and hygroscopic growth, and supports the goals of the RHR by reducing biases in visibility trends.

Acknowledgment

IMPROVE is a collaborative association of state, tribal, and federal agencies, and international partners. The U.S. Environmental Protection Agency (EPA) is the primary funding source, with contracting and research support from the National Park Service. The Air Quality Research Center at the University of California, Davis, is the central analytical laboratory, with ion analysis provided by the Research Triangle Institute, and carbon analysis provided by the Desert Research Institute. Support of the optical network is provided by Air Resources, Inc. Bonne Ford used GPT-5 for coding assistance in the generation of figures (Figures S5, S11, S14, and S16).

Disclosure statement

No potential conflict of interest was reported by the author(s).

Funding

This work was funded by the National Park Service Air Resources Division under task agreement number [P24ACO2378-0] under Cooperative Agreement [P22AM01168]. Views presented herein are those of the authors and should not be interpreted as necessarily representing the National Park Service.

About the authors

Bonne Ford is a research scientist at the Cooperative Institute for Research in the Atmosphere at Colorado State University.

Anthony J. Prenni is the research and monitoring branch lead of the Air Resources Division for the National Park Service.

Willliam Malm is a senior research scientist at the Cooperative Institute for Research in the Atmosphere at Colorado State University.

Scott A. Copeland is a research associate at the Cooperative Institute for Research in the Atmosphere at Colorado State University.

Bret A. Schichtel is a physical scientist with the Air Resources Division for the National Park Service.

Jenny Hand is a senior research scientist at the Cooperative Institute for Research in the Atmosphere at Colorado State University.

ORCID

Bonne Ford http://orcid.org/0000-0002-7045-8346
Bret A. Schichtel http://orcid.org/0000-0002-5512-8082
Jenny Hand http://orcid.org/0000-0002-4644-2459

Data availability statement

All IMPROVE filter and Optec nephelometer data used in this study are available through the Federal Land Manager Environmental Database (FED, https://views.cira.colostate.edu/fed/). Automated data processing procedures are under development for the 2-WIN data and will be made available on FED in 2026. Until the completion of those procedures, the data are available upon request.

References

Ames RB, Hand JL, Kreidenweis SM, Day DE, Malm WC. 2000. Optical measurements of aerosol size distributions in Great Smoky Mountains National Park: dry aerosol characterization. J Air Waste Manag Assoc. 50(5):665–676. https://doi.org/10.1080/10473289.2000.10464128

Brock CA et al. 2016. Aerosol optical properties in the southeastern United States in summer – part 1: hygroscopic growth. Atmos Chem Phys. 16(8):4987–5007. https://doi.org/10.5194/acp-16-4987-2016

DeBell LJ et al. 2006. Spatial and seasonal patterns and temporal variability of haze and its constituents in the United States report IV (no. IV). Cooperative Institute for Research in the Atmosphere, Colorado State University.

Dusek U et al. 2010. Enhanced organic mass fraction and decreased hygroscopicity of cloud condensation nuclei (CCN) during new particle formation events. Geophys Res Lett. 37. https://doi.org/10.1029/2009GL040930

Gantt B, Beaver M, Timin B, Lorang P. 2018. Recommended metric for tracking visibility progress in the regional haze rule. J Air Waste Manag Assoc. 68(5):438–445. https://doi.org/10.1080/10962247.2018.1424058

Gordon TD et al. 2018. Open-path, closed-path, and reconstructed aerosol extinction at a rural site. J Air Waste Manag Assoc. 68:824–835. https://doi.org/10.1080/10962247.2018.1452801

Gunthe SS et al. 2009. Cloud condensation nuclei in pristine tropical rainforest air of Amazonia: size-resolved measurements and modeling of atmospheric aerosol composition and CCN activity. Atmos Chem Phys. 9(19):7551–7575. https://doi.org/10.5194/acp-9-7551-2009

Hand JL et al. 2023. Spatial and seasonal patterns and temporal variability of haze and its constituents in the United States report VI (no. VI). Cooperative Institute for Research in the Atmosphere, Colorado State University.

Hand JL et al. 2024. Spatial and seasonal variability of remote and urban speciated fine particulate matter in the United States. J Geophys Res. 129(23):e2024JD042579. https://doi.org/10.1029/2024JD042579

Hand JL, Malm WC. 2007. Review of aerosol mass scattering efficiencies from ground-based measurements since 1990. J Geophys Res. 112(D16). https://doi.org/10.1029/2007JD008484

Hand JL, Prenni AJ, Copeland S, Schichtel BA, Malm WC. 2020. Thirty years of the Clean Air Act Amendments: Impacts on haze in remote regions of the United States (1990–2018). Atmos Environ. 243:117865. https://doi.org/10.1016/j.atmosenv.2020.117865

Hand JL, Prenni AJ, Schichtel BA, Malm WC, Chow JC. 2019. Trends in remote PM2.5 residual mass across the United States: Implications for aerosol mass reconstruction in the IMPROVE network. Atmos Environ. 203:141–152. https://doi.org/10.1016/j.atmosenv.2019.01.049

Haslett SL et al. 2019. The radiative impact of out-of-cloud aerosol hygroscopic growth during the summer monsoon in Southern West Africa. Atmos Chem Phys. 19(3):1505–1520. https://doi.org/10.5194/acp-19-1505-2019

Japar SM et al. 1984. Comparison of colvent extraction and thermal-optical carbon analysis methods: Application to diesel vehicle exhaust aerosol. Environ Sci Technol. 18(4):231–234. https://doi.org/10.1021/es00122a004

Jimenez JL et al. 2009. Evolution of organic aerosols in the atmosphere. Science (New York, NY). 326:1525–1529. https://doi.org/10.1126/science.1180353

Laing JR, Jaffe DA, Hee JR. 2016. Physical and optical properties of aged biomass burning aerosol from wildfires in Siberia and the western USA at the Mt. Bachelor observatory. Atmos Chem Phys. 16:15185–15197. https://doi.org/10.5194/acp-16-15185-2016

Latimer RNC, Martin RV. 2019. Interpretation of measured aerosol mass scattering efficiency over North America using a chemical transport model. Atmos Chem Phys. 19(4):2635–2653. https://doi.org/10.5194/acp-19-2635-2019

Lowenthal D et al. 2015. Evaluation of assumptions for estimating chemical light extinction at U.S. national parks. J Air Waste Manag Assoc. 65:249–260. https://doi.org/10.1080/10962247.2014.986307

Lowenthal DH et al. 2003. Hygroscopic organic aerosols during BRAVO? J Air Waste Manag Assoc. 53:1273–1279. https://doi.org/10.1080/10473289.2003.10466284

Lowenthal DH, Kumar N. 2004. Variation of mass scattering efficiencies in IMPROVE. J Air Waste Manag Assoc. 54:926–934. https://doi.org/10.1080/10473289.2004.10470969

Lowenthal DH, Kumar N. 2016. Evaluation of the improve equation for estimating aerosol light extinction. J Air Waste Manag Assoc. 66:726–737. https://doi.org/10.1080/10962247.2016.1178187

Malm WC et al. 2000. Spatial and seasonal patterns and temporal variability of haze and its constituents in the United States: Report iii. Coop. Inst. for Res. Colo. State Univ.

Malm WC et al. 2005. Intercomparison and closure calculations using measurements of aerosol species and optical properties during the yosemite aerosol characterization study. J Geophys Res. 110(D14). https://doi.org/10.1029/2004JD005494

Malm WC et al. 2024. Revisiting integrating nephelometer measurements. Atmos Environ. 319:120237. https://doi.org/10.1016/j.atmosenv.2023.120237

Malm WC, Day DE. 2001. Estimates of aerosol species scattering characteristics as a function of relative humidity. Atmos Environ. 35:2845–2860. https://doi.org/10.1016/S1352-2310(01)00077-2

Malm WC, Day DE, Kreidenweis SM, Collett JL, Lee T. 2003. Humidity-dependent optical properties of fine particles during the big bend regional aerosol and visibility observational study. J. Geophys. Res. 108(D9):4279. https://doi.org/10.1029/2002JD002998

Malm WC, Hand JL. 2007. An examination of the physical and optical properties of aerosols collected in the

IMPROVE program. Atmos Environ. 41:3407–3427. https://doi.org/10.1016/j.atmosenv.2006.12.012

Malm WC, Molenar JV, Eldred RA, Sisler JF. 1996. Examining the relationship among atmospheric aerosols and light scattering and extinction in the Grand Canyon area. J Geophys Res. 101(D14):19251–19265. https://doi.org/10.1029/96JD00552

Malm WC, Pitchford ML. 1997. Comparison of calculated sulfate scattering efficiencies as estimated from size-resolved particle measurements at three national locations. Atmos Environ. 31:1315–1325. https://doi.org/10.1016/S1352-2310(96)00280-4

Malm WC, Sisler JF. 2000. Spatial patterns of major aerosol species and selected heavy metals in the United States. Fuel Process Technol. 65–66:473–501. https://doi.org/10.1016/S0378-3820(99)00111-3

Malm WC, Sisler JF, Huffman D, Eldred RA, Cahill TA. 1994. Spatial and seasonal trends in particle concentration and optical extinction in the United States. J Geophys Res. 99 (D1):1347–1370. https://doi.org/10.1029/93JD02916

Marsavin A et al. 2023. Optical properties of biomass burning aerosol during the 2021 Oregon fire season: comparison between wild and prescribed fires. Environ Sci: Atmos. 3 (3):608–626. https://doi.org/10.1039/D2EA00118G

Molenar JV. 1997. Analysis of the real world performance of the Optec NGN-2 ambient nephelometer. In: Visual air quality: aerosols and global radiation balance. Presented at the Air and Waste Management Association. p 243–265.

Molenar JV. 2000. Theoretical analysis of $PM_{2.5}$ mass measurements by Nephelometry. In: Proceedings of PM2000: Particulate Matter and Health. Presented at the Air & Waste Management Association.

Müller T, Laborde M, Kassell G, Wiedensohler A. 2011. Design and performance of a three-wavelength LED-based total scatter and backscatter integrating nephelometer. Atmos Meas Tech. 4(6):1291–1303. https://doi.org/10.5194/amt-4-1291-2011

Petters MD, Kreidenweis SM. 2007. A single parameter representation of hygroscopic growth and cloud condensation nucleus activity. Atmos Chem Phys. 7(8):1961–1971. https://doi.org/10.5194/acp-7-1961-2007

Pierce JR et al. 2011. Quantification of the volatility of secondary organic compounds in ultrafine particles during nucleation events. Atmos Chem Phys. 11(17):9019–9036. https://doi.org/10.5194/acp-11-9019-2011

Pitchford M et al. 2007. Revised algorithm for estimating light extinction from improve particle speciation data. J Air Waste Manag Assoc. 57:1326–1336. https://doi.org/10.3155/1047-3289.57.11.1326

Pitchford ML, Malm WC. 1994. Development and applications of a standard visual index. Atmospheric Environment, Conference on visibility and fine particles 28:1049–1054. https://doi.org/10.1016/1352-2310(94)90264-X

Prenni AJ et al. 2019. An examination of the algorithm for estimating light extinction from IMPROVE particle speciation data. Atmos Environ. 214:116880. https://doi.org/10.1016/j.atmosenv.2019.116880

Prenni AJ, Petters MD, Kreidenweis SM, DeMott PJ, Ziemann PJ. 2007. Cloud droplet activation of secondary organic aerosol. J Geophys Res. 112(D10). https://doi.org/10.1029/2006JD007963

Pringle KJ, Tost H, Pozzer A, Pöschl U, Lelieveld J. 2010. Global distribution of the effective aerosol hygroscopicity parameter for CCN activation. Atmos Chem Phys. 10 (12):5241–5255. https://doi.org/10.5194/acp-10-5241-2010

Quinn PK, Kapustin VN, Bates TS, Covert DS. 1996. Chemical and optical properties of marine boundary layer aerosol particles of the mid-Pacific in relation to sources and meteorological transport. J. Geophys. Res. 101 (D3):6931–6951. https://doi.org/10.1029/95JD03444

Quinn PK, Marshall SF, Bates TS, Covert DS, Kapustin VN. 1995. Comparison of measured and calculated aerosol properties relevant to the direct radiative forcing of the tropospheric sulfate aerosol on climate. J. Geophys. Res. 100(D5):8977–8991. https://doi.org/10.1029/95JD00387

Ryan PA, Lowenthal D, Kumar N. 2005. Improved light extinction reconstruction in interagency monitoring of protected visual environments. J Air Waste Manag Assoc. 55(11):1751–1759. https://doi.org/10.1080/10473289.2005.10464768

Tang IN. 1997. Thermodynamic and optical properties of mixed-salt aerosols of atmospheric importance. J. Geophys. Res. 102:1883–1893. https://doi.org/10.1029/96JD03085

Trijonis J et al. others. 1987. Preliminary extinction budget results from the resolve program. In: Transactions, visibility protection: research and policy aspects; Air Pollution Control Association. p 872–883.

U.S. Environmental Protection Agency. 1999. Visibility monitoring guidance (EPA-454/R-99-003).

U.S. Environmental Protection Agency. 2003. Guidance for tracking progress under the regional haze rule (EPA-454/B-03-004).

U.S. Environmental Protection Agency. 2018. Technical guidance on tracking visibility progress for the second implementation period of the regional haze program (EPA-454/R-18-010).

Zieger P et al. 2017. Revising the hygroscopicity of inorganic sea salt particles. Nat Commun. 8(1). https://doi.org/10.1038/ncomms15883